INVITED REVIEW

Modulation of cyclic nucleotide-regulated HCN channels by PIP$_2$ and receptors coupled to phospholipase C

Phillip Pian · Annalisa Bucchi · Anthony DeCostanzo · Richard B. Robinson · Steven A. Siegelbaum

Abstract Recent results indicate that phosphoinositides, including phosphatidylinositol 4,5-bisphosphate (PI(4,5)P$_2$), directly enhance the opening of hyperpolarization-activated, cyclic nucleotide-regulated (HCN) channels by shifting their activation gating to more positive voltages. This contrasts with the action of phosphoinositides to inhibit the opening of the related cyclic nucleotide-gated (CNG) channels involved in sensory signaling. We both review previous studies and present new experiments that investigate whether HCN channels may be regulated by dynamic changes in PI(4,5)P$_2$ levels caused by the receptor-mediated activation of phospholipase C (PLC). We coexpressed HCN1 or HCN2 channels in *Xenopus* oocytes with the PLC-coupled bradykinin BK$_2$ receptor, the muscarinic M1 receptor, or the TrkA receptor. Activation of all three receptors produced a positive shift in HCN channel voltage gating, the opposite of the effect expected for PI(4,5)P$_2$ depletion. This action was not caused by alterations in cAMP as the effect was preserved in HCN mutant channels that fail to bind cAMP. The receptor effects were mediated by PLC activity, but did not depend on signaling through the downstream products of PI(4,5)P$_2$ hydrolysis: IP$_3$ or diacylglycerol (DAG). Importantly, the modulatory effects on gating were blocked by inhibitors of phosphatidylinositol (PI) kinases, suggesting a role for increased PI(4,5)P$_2$ synthesis. Finally, we found that bradykinin exerted a similar PI kinase-dependent effect on the gating of native HCN channels in cardiac sinoatrial node cells, suggesting that this pathway may represent a novel, physiologically relevant mechanism for enhancing HCN channel function.

P. Pian · S. A. Siegelbaum
Center for Neurobiology and Behavior,
Columbia University Medical Center,
New York, NY 10032, USA

A. Bucchi · A. DeCostanzo · R. B. Robinson · S. A. Siegelbaum
Department of Pharmacology,
Columbia University Medical Center,
New York, NY 10032, USA

R. B. Robinson
Center for Molecular Therapeutics,
Columbia University Medical Center,
New York, NY 10032, USA

S. A. Siegelbaum
Howard Hughes Medical Institute,
Columbia University Medical Center,
New York, NY 10032, USA

S. A. Siegelbaum (✉)
1051 Riverside Drive; P.I. Annex Room 625,
New York, NY 10032, USA
e-mail: sas8@columbia.edu

Introduction

Since the pioneering work of Hilgemann and Ball demonstrated modulatory effects of phosphatidylinositol 4,5-bisphosphate (PI(4,5)P$_2$) on the Na$^+$–Ca^{2+} exchanger and the ATP-sensitive K$_{ATP}$ channel [25], many other channels and transporters have been identified as targets of phosphoinositide (PI) modulation [66]. Below we summarize recent results demonstrating that PI(4,5)P$_2$ and related phosphoinositides have a direct modulatory effect on two families of ion channels that are directly regulated by the binding of cyclic nucleotides to a C-terminal cyclic nucleotide-binding domain (CNBD). These include the cyclic nucleotide-gated (CNG) channels important for

visual and olfactory signal transduction [14] and the hyperpolarization-activated, cyclic nucleotide-regulated, cation-nonselective (HCN) channels that generate the hyperpolarization-activated currents (I_f or I_h) important for cardiac and neuronal pacemaker activity [61].

Despite considerable evidence that CNG and HCN channels are regulated by both endogenous and exogenous polyphosphoinositides, it is not clear whether this mechanism is utilized by cell signaling pathways to dynamically control the activity of these channels. In this paper we provide new experimental results demonstrating that stimulation of receptors coupled to phospholipase C (PLC) and hydrolysis of PI(4,5)P$_2$ indeed modulate the gating of both recombinant and native HCN channels. Surprisingly, the effect on HCN channel gating of stimulating PLC activity is similar to the effect of direct application of PI(4,5)P$_2$ to the channel [51, 92]. Our results suggest that these receptor-mediated PLC-dependent actions result from a net increase in local PI(4,5)P$_2$ levels near the HCN channels due to the stimulation of polyphosphoinositide synthesis through PI kinase activity.

Previous studies of PI(4,5)P$_2$ modulation of CNG channels

It has been known for some time that invertebrate phototransduction involves the activation of PLC and cleavage of PI(4,5)P$_2$ into inositol trisphosphate (IP$_3$) and diacylglycerol (DAG) [59]. Based on the modulatory effects of PI(4,5)P$_2$ on various ion channels and the known role of CNG channels in phototransduction, Womack et al. [80] investigated the possible role of PI(4,5)P$_2$ in CNG channel regulation. Indeed, these authors found that PI(4,5)P$_2$ exerted a strong inhibitory effect on heteromeric CNG channels formed from bovine rod CNGA1 and CNGB1 subunits coexpressed in *Xenopus* oocytes. PI(4,5)P$_2$ decreased the maximal response of the recombinant CNG channels to a saturating concentration of cyclic nucleotide by approximately 50%. A similar inhibitory effect of the lipid was observed on native CNG currents in membrane patches from rod outer segments.

The inhibitory effect of PI(4,5)P$_2$ was mimicked by application of MgATP to inside-out patches and this action was blocked by inclusion of an anti-PI(4,5)P$_2$ monoclonal antibody in the bath solution. These results suggest that MgATP acts to promote phosphorylation of phosphatidylinositol, leading to an increase in PI(4,5)P$_2$ levels [80]. A similar inhibitory effect of MgATP was observed in rod outer segments.

Although Womack et al. [80] found no effect of PI(4,5)P$_2$ on olfactory CNG channels, Zhainazarov et al. [86] reported that both recombinant and native olfactory CNG channels were inhibited by PI(3,4,5)P$_3$. The inhibitory effect of PI(3,4,5)P$_3$ was mapped to a 30-amino-acid stretch in the N terminus of the olfactory CNGA2 subunit that contains a region that also binds Ca^{2+}/calmodulin [12, 72]. Binding of PI(3,4,5)P$_3$ to the channel occluded the normal inhibitory effects of Ca^{2+}/calmodulin on both homomeric CNGA2 channels and heteromeric CNG channels expressed from cloned CNGA2/A4 and CNGB1b subunits. In contrast, homomeric CNGA3 subunits were not affected by PI(3,4,5)P$_3$.

PI(4,5)P$_2$ modulation of HCN channels

Although the opening of both CNG and HCN channels is enhanced by cyclic nucleotides, the two channels exhibited a strikingly different response to PI(4,5)P$_2$. Whereas PI(4,5)P$_2$ and PI(3,4,5)P$_3$ inhibited the opening of CNG channels, as discussed above, both phospholipids potentiated the opening of recombinant HCN channels expressed in *Xenopus* oocytes, owing to a shift in the voltage-dependence of channel activation to more positive potentials [51, 92]. PI(4,5)P$_2$ also altered the kinetics of HCN channel gating, with a slowing of both opening rate during large hyperpolarizing steps and closing rate after return of the membrane to −40 mV [51]. The extent of the voltage shift with a short-chain synthetic PI(4,5)P$_2$ analog showed a saturating dependence on phosphoinositide concentration. Interestingly, the depolarizing shift in response to exogenous PI(4,5)P$_2$ was the opposite of the hyperpolarizing shift in HCN channel gating that occurs during rundown associated with whole-cell recordings or recordings from cell-free patches. As PI(4,5)P$_2$ depletion by membrane bound lipid phosphatases had been suggested to underlie rundown of other types of channels [66, 82, 88], we [51] and others [92] investigated the hypothesis that the rundown of HCN channels is caused by a similar mechanism.

Several lines of evidence support the idea that depletion of PI(4,5)P$_2$ underlies rundown. Thus, application of an anti-PI(4,5)P$_2$ antibody to HCN channels in inside-out patches enhanced rundown by producing an even greater hyperpolarizing shift in channel gating [51]. Conversely, blockade of phosphatases slowed the hyperpolarizing shift seen upon patch excision [51, 92]. Finally, rundown was partially reversed by application of MgATP to inside-out patches, which shifted HCN activation gating in the depolarizing direction, similar to the action of PI(4,5)P$_2$. The effect of MgATP was shown to be caused by an enhancement in phosphatidylinositol phosphorylation as its effects were blocked by wortmannin, an inhibitor of PI kinases [51]. The voltage shift with both PI(4,5)P$_2$ and rundown appears to reflect changes in internal membrane surface charge as intracellular application of the poly-cation poly-lysine, which screens negative surface charge, enhanced the rate of channel rundown [51] and abolished the effect of exogenously applied PI(4,5)P$_2$ [92].

Although both $PI(4,5)P_2$ and cAMP exert similar facilitatory effects on HCN channel opening by shifting gating to more positive voltages, several results suggest that the two molecules act through distinct mechanisms. First, the effects of $PI(4,5)P_2$ either failed to occlude [92] or only partially occluded [51] the actions of cAMP to enhance gating. Second, blockade of the action of cAMP by either deletion of the HCN2 cyclic nucleotide-binding domain (CNBD) or a point mutation (R591E) had no effect on the facilitatory action of $PI(4,5)P_2$ [51, 92]. Third, the efficacy of cAMP and $PI(4,5)P_2$ varied independently among different channel subtypes. Thus, whereas the gating of HCN4 was shifted by a similar extent by the two ligands, the gating of HCN1 was shifted to a much greater extent by $PI(4,5)P_2$ compared to cAMP.

$PI(4,5)P_2$ was also found to act as an endogenous modulator of the gating of native HCN channels. Thus, rundown of HCN currents during whole-cell recordings from rabbit sinoatrial node cells [51] and embryonic cardiomyocytes [92] was greatly slowed by inclusion of $PI(4,5)P_2$ in the recording pipette. Moreover, in perforated-patch whole-cell recordings from dopaminergic neurons of the substantia nigra (DA-SN), bath application of wortmannin caused a hyperpolarizing shift in HCN current gating that was accompanied by a 30–40% decrease in the firing rate of DA-SN neurons [92]. Thus, both cardiac and neuronal pacemaking activity may be regulated by a constitutive action of $PI(4,5)P_2$ to enhance HCN channel opening.

PLC modulation of ion channels

The above evidence provides strong support for the idea that CNG and HCN channels are regulated by both exogenous and endogenous polyphosphoinositides, and that, at least for HCN channels, the loss of this endogenous modulation can contribute to channel rundown. However, the physiological significance of this regulation is far less clear. Are CNG or HCN channels also modulated by dynamic changes in phospholipid content of the membrane associated with receptor-mediated signaling? Or does the regulation by $PI(4,5)P_2$ represent an invariant, constitutive action under normal physiological conditions?

A large number of ion channels are regulated by cell surface receptors that activate PLC [20, 36, 67, 74]. This enzyme hydrolyzes $PI(4,5)P_2$, leading to regional decreases in $PI(4,5)P_2$ levels in the membrane and the generation of the second messengers, IP_3 and DAG [7, 26]. The latter two molecules can either modulate ion channels by directly binding to them or by activating downstream signaling cascades. Cell signaling via IP_3 is mediated by the release of Ca^{2+} from intracellular stores [47], whereas signaling via DAG is mediated by its binding to the regulatory C_1

domain found in proteins with diverse functions [8], including protein kinase C [75] and DAG kinase [71]. Although it has long been known that the IP_3 receptor is a Ca^{2+} channel [18, 46, 50], DAG may also directly bind to and activate channels, as demonstrated for the transient receptor potential channels (TRPCs) [27]. Moreover, recent experiments have demonstrated that the opening of HCN channels is enhanced by an effect of phorbol esters to stimulate both PKC and DAG kinase, leading to a cascade of downstream signaling events that are likely to involve direct effects of phosphatidic acid and arachidonic acid on the HCN channels [17].

In addition to signaling through IP_3 and DAG production, receptor-mediated activation of PLC can also lead to changes in channel function because of the loss of a basal modulatory action of $PI(4,5)P_2$ caused by its hydrolysis [66]. This mechanism mediates the suppression of the KCNQ/M current by muscarinic ACh agonists [65, 67, 79, 87], the inhibition of N-type voltage-gated calcium channels by luteinizing hormone-releasing hormone [82] and muscarinic agonists [19] in sympathetic neurons, and the upregulation of TRPV1 current during hyperalgesia in trigeminal sensory neurons [13].

In *Xenopus* oocytes, activation of heterologously expressed PLC-linked receptors has been shown to modulate a number of $PI(4,5)P_2$-sensitive recombinant channels, including GIRK channels [32], TRPV1 [13], and voltage-gated Ca^{2+} channels [82]. The time scale of receptor modulation varies from as rapidly as ~50 s for the maximal suppression of KCNQ2/3 current by activation of the bradykinin BK_2 receptor [87], to as slowly as 25 min for the maximal inhibition of P/Q-type calcium channels by stimulation of the nerve growth factor (NGF) TrkA receptor [82].

In some instances, stimulation of PLC can activate downstream signaling pathways that increase $PI(4,5)P_2$ synthesis [6, 31, 55, 57, 62, 68, 83]. Regional and global levels of cellular $PI(4,5)P_2$ thus reflect the balance between $PI(4,5)P_2$ synthesis and cleavage, and the net steady-state effect of receptor stimulation on $PI(4,5)P_2$ levels varies by receptor and cell type. For example, activation of both muscarinic M1 and bradykinin BK_2 receptors stimulates PLC and inhibits the opening of M-type K^+ channels [29] and N-type Ca^{2+} channels [19] in sympathetic neurons. However, M1 receptor stimulation produces a much greater depletion of $PI(4,5)P_2$ levels compared to that achieved with BK, because of the Ca^{2+}-dependent action of BK to stimulate $PI(4,5)P_2$ synthesis [19, 29]. In cardiac atrial muscle, activation of PLC by muscarinic agonists fails to alter total $PI(4,5)P_2$ concentration [49, 56], indicating a balance of lipid hydrolysis and synthesis.

In yet other cell types, an enhancement in synthesis of $PI(4,5)P_2$ upon receptor-mediated PLC activation can out-

weigh its direct cleavage by PLC, resulting in a net increase in PI(4,5)P$_2$ levels. Thus, global increases in PI(4,5)P$_2$ are seen in *Xenopus* oocytes after fertilization [63], as well as in platelets after exposure to thrombin [35]. A local increase of PI(4,5)P$_2$ levels within membrane ruffles has also been reported in HeLa cells after EGFR activation [28].

PLC modulation of HCN channels

In this study, we investigated the effects of receptor-mediated PLC activation on HCN channel function in *Xenopus* oocytes and sinoatrial node myocytes. Based on the findings that both endogenous and exogenous PI(4,5)P$_2$ enhanced HCN channel opening by shifting activation to more positive potentials [51, 92], we expected that receptor-mediated stimulation of PLC would produce a hyperpolarizing shift in HCN activation owing to a depletion in PI(4,5)P$_2$. Surprisingly, we found that stimulation of a variety of cell surface receptors linked to PLC enhanced the activation of both recombinant HCN channels expressed in *Xenopus* oocytes and native HCN channels in cardiac sinoatrial myocytes by shifting voltage-gating in the positive direction, the opposite to the effect expected for PI(4,5)P$_2$ depletion. The voltage shift was also accompanied by a slowing of channel closing kinetics. These changes were not mediated by direct binding of IP$_3$ or DAG to the channel. Nor did they depend on an increase in intracellular Ca^{2+}, activation of protein kinases, including PKC, or activation of other proteins with regulatory C$_1$ domains.

The PLC-dependent modulation of HCN channels was, however, inhibited by the PI kinase inhibitors wortmannin and LY294002, at concentrations required to block PI 4-kinases. These results are consistent with the idea that the HCN channels are regulated by a local pool of PI(4,5)P$_2$ that may be enhanced after receptor-mediated activation of PLC.

Materials and methods

Expression in *Xenopus* oocytes

Mouse HCN1 and HCN2 were previously cloned into pGHE19 and pGEMHE, respectively, and the HCN2$_{R591E}$ mutant was previously constructed [11]. M1 AChR and the BK$_2$ receptor in the pGEMHE vector or its derivatives were the generous gift of Diomedes Logothetis (Mount Sinai School of Medicine); p75, TrkA, TrkA Y499F, and TrkA Y794F in pGEMHE derivatives were kindly supplied by Jian Yang (Columbia University); linearized RNA for the α_{1A} and β_1 subunits of the P/Q type voltage-gated calcium channel was the generous gift of Geoffrey Pitt (Columbia University). cRNA was transcribed from linearized DNA using T7 RNA polymerase (mMessage mMachine; Ambion) and injected into *Xenopus* oocytes as described previously [22]. Oocytes were injected with 5 ng of HCN1 or HCN2 cRNA; in coexpression experiments, oocytes were injected with 20 ng of HCN and 20 ng of receptor cRNA. Expression of TrkA and its mutants required injection of 15 ng of p75, 15 ng of TrkA, and 16.5 ng of HCN2$_{R591E}$.

Xenopus oocyte electrophysiological recordings

Two-microelectrode voltage-clamp recordings were obtained 1 day after cRNA injection using an oocyte voltage-clamp amplifier (model OC-725C, Warner Instruments). Data were filtered at 1 kHz and sampled at 2 kHz. The recordings were obtained with the oocytes bathed in an extracellular solution containing (in mM): 96 KCl, 2 NaCl, 10 HEPES, and 2 MgCl$_2$, pH 7.5. Microelectrodes were filled with 3 M KCl and had resistances of 0.5–2 MΩ.

Cell-free inside-out patches were obtained 5–6 days after cRNA injection, and data were acquired using a patch-clamp amplifier (Axopatch 200B; Axon Instruments). Patch pipettes had resistances of 1–3 MΩ and were filled with a pipette solution containing (in mM): 96 KCl, 1 NaCl, 10 HEPES, 1.8 CaCl$_2$, and 1 MgCl$_2$, pH 7.4. The bath solution contained: 96 KCl, 1 NaCl, 10 HEPES, and 5 EGTA, pH 7.4. An Ag–AgCl ground wire was connected to the bath solution by a 3-M KCl agar bridge electrode, and junction potential was compensated before the formation of each patch. Linear leak currents were not subtracted. Data were filtered at 1 kHz with an eight-pole low-pass Bessel filter (Frequency Devices) and sampled at 2 kHz with an ITC-16 interface (Instrutech) and Pulse software (HEKA).

Hyperpolarizing voltages in −10-mV step increments were applied to either inside-out patches or intact oocytes from a holding potential of −30 mV. All recordings were obtained at room temperature (18–22°C).

Data analysis

HCN currents were analyzed as previously described [11]. Activation curves were determined from plots of tail current amplitude (measured at −40 mV) as a function of test voltage during 3-s long hyperpolarizing steps. Activation curves were fit with a Boltzmann equation to obtain the midpoint voltage of activation ($V_{1/2}$) and slope factor (s) of the relation (both in units of mV). Analysis was done using PulseFit (HEKA), Excel (Microsoft), and Origin (Microcal). Single comparisons between two experimental conditions were evaluated by a Student's t test. Comparisons involving multiple populations were evaluated by ANOVA with a Scheffe Post hoc test.

Experiments on rabbit sinoatrial node cells

Animal protocols conformed to the guidelines of the care and use of laboratory animals established by U.S. (National Institutes of Health publication No. 85-23) directives. Single sinoatrial node cells were isolated from young New Zealand rabbits (0.8–1.2 kg) as previously described [15]. Patch clamp analysis was performed in the whole-cell configuration at 34°C. The pipette was filled with (in mM): 130 aspartic acid, 146 KOH, 10 NaCl, 2 $CaCl_2$, 5 EGTA-KOH, 2 Mg-ATP, and 10 HEPES-KOH, pH 7.2. The external Tyrode's solution used to record I_h contained (in mM): 140 NaCl, 2.3 NaOH, 1 $MgCl_2$, 5.4 KCl, 1.8 $CaCl_2$, 5 HEPES, 10 glucose, 2 $MnCl_2$, and 1 $BaCl_2$, pH 7.4. When indicated, bradykinin (100 nM) and wortmannin (10 μM) were added separately or together to the Tyrode's solution. Before the recording, cells were incubated at 34°C for 30 min with bradykinin or for 60 min with wortmannin. For experiments in which the effect of the two substances was evaluated in the same cell, bradykinin was added to the bath solution after a 30-min preincubation with wortmannin.

The I_h activation curve was obtained using a two-voltage step protocol in which hyperpolarizing steps (−25 to −130 mV) from a holding potential of −25 mV were applied followed by a step to −70 mV to measure the tail current. The duration of the activation steps varied with the test voltage to allow activation to reach a steady-state value. Plots of normalized tail current amplitude as a function of test voltage were fit with a Boltzmann function to obtain the $V_{1/2}$ and slope factor. Time constants were calculated by fitting the first part of the activation and deactivation current traces by a single exponential function after an initial delay. Currents were recorded and filtered on-line at 1 kHz with an Axopatch 200B amplifier, and acquired using pClamp 9.0 software (Axon Instruments). Values are given as the mean±SEM and data were compared using the Student's t test. Values of $P<0.05$ were considered significant.

Reagents and drugs

U73122 and U73343 (Calbiochem) were reconstituted in HPLC grade chloroform (Sigma-Aldrich), aliquoted in single-use volumes, and evaporated under a stream of nitrogen. Stock solutions of all other water-insoluble reagents were prepared in DMSO, stored at −20°C and diluted to appropriate final concentrations before use. We used the following additional reagents: wortmannin, LY294002, BAPTA-AM, R59949, and erbstatin analog (Biomol); bradykinin (Bachem); 7s nerve growth factor purified from mouse brain (Roche); SAG, PDBu, RO 31-8220, and staurosporine (Calbiochem). All other reagents were acquired from Sigma-Aldrich.

Results

BK_2 receptor activation alters HCN gating in *Xenopus* oocytes

The receptor-dependent, PLC-mediated regulation of HCN channels was initially studied by coexpressing in *Xenopus* oocytes either HCN1 or HCN2 with the bradykinin BK_2 receptor, which is coupled to the $G_{q/11}$-dependent stimulation of PLCβ. Exposure of the oocytes to 100 nM bradykinin led to the transient activation of an endogenous calcium-activated Cl^- current, $I_{Cl,Ca}$, an effect previously shown to result from the IP_3-dependent release of Ca^{2+} from oocyte intracellular stores [21]. The Cl^- current reached a peak value within 30 s and then decayed back to baseline within 90 s (data not shown).

After decay of the Cl^- current, HCN1 and HCN2 currents were measured in response to a series of 3-s-long hyperpolarizing voltage steps to various potentials. BK_2 receptor activation caused a marked change in the hyperpolarization-activated currents generated by both HCN1 and HCN2 (Fig. 1). However, rather than shifting activation in the hyperpolarizing direction, as expected for a PLC-mediated decrease in $PI(4,5)P_2$ levels [51, 92], bradykinin shifted the voltage dependence of gating of both channels in the depolarizing direction (Fig. 1c,d; Fig. 2a). In contrast to this facilitatory effect on channel gating, bradykinin also decreased the maximal HCN tail current amplitude after a hyperpolarizing step to extreme negative voltages where voltage-dependent activation had reached completion (Fig. 1a,b; Fig. 2b). This effect suggests a decrease in the number of functional channels in the membrane or a decrease in maximal channel open probability. Bradykinin also produced a twofold slowing in the time course of channel deactivation, as measured by the rate of tail current decay (Table 1), with relatively little effect on the rate of channel activation.

Bradykinin exerted qualitatively similar effects on the gating of HCN1 and HCN2 (Figs. 1c,d; 2a). However, the extent of the shift in gating, measured by the change in the voltage at which channels are half-activated ($\Delta V_{1/2}$), was significantly greater for HCN2 ($\Delta V_{1/2}=18.9\pm2.0$ mV, mean±SEM) than for HCN1 ($\Delta V_{1/2}=6.9\pm1.3$ mV; $P<0.001$; ANOVA, Post hoc). In contrast, the extent to which BK suppressed the maximal tail current amplitude was somewhat greater for HCN1 than for HCN2 (Fig. 2b; $P<0.08$; ANOVA, Post hoc). Finally, the effect of bradykinin to slow the time course of tail current deactivation was greater for HCN2 than HCN1 (Table 1). Thus, BK_2 receptor stimulation

Fig. 1 Activation of type 2 bradykinin receptor (BK$_2$) alters wild-type HCN1 and HCN2 gating and current amplitude. **a** and **b** Macroscopic HCN1 (**a**) and HCN2 (**b**) currents shown for individual oocytes in response to a series of hyperpolarizing voltage steps before (*left*) and after (*right*) 28.5 min of incubation in bradykinin. **c** and **d** Mean normalized tail currents for HCN1 (*n*=5) and HCN2 (*n*=7) plotted as a function of test potential and fit with the Boltzmann equation. Data obtained before (*filled circles*) or after (*open circles*) bradykinin exposure. *Error bars* indicate SEM
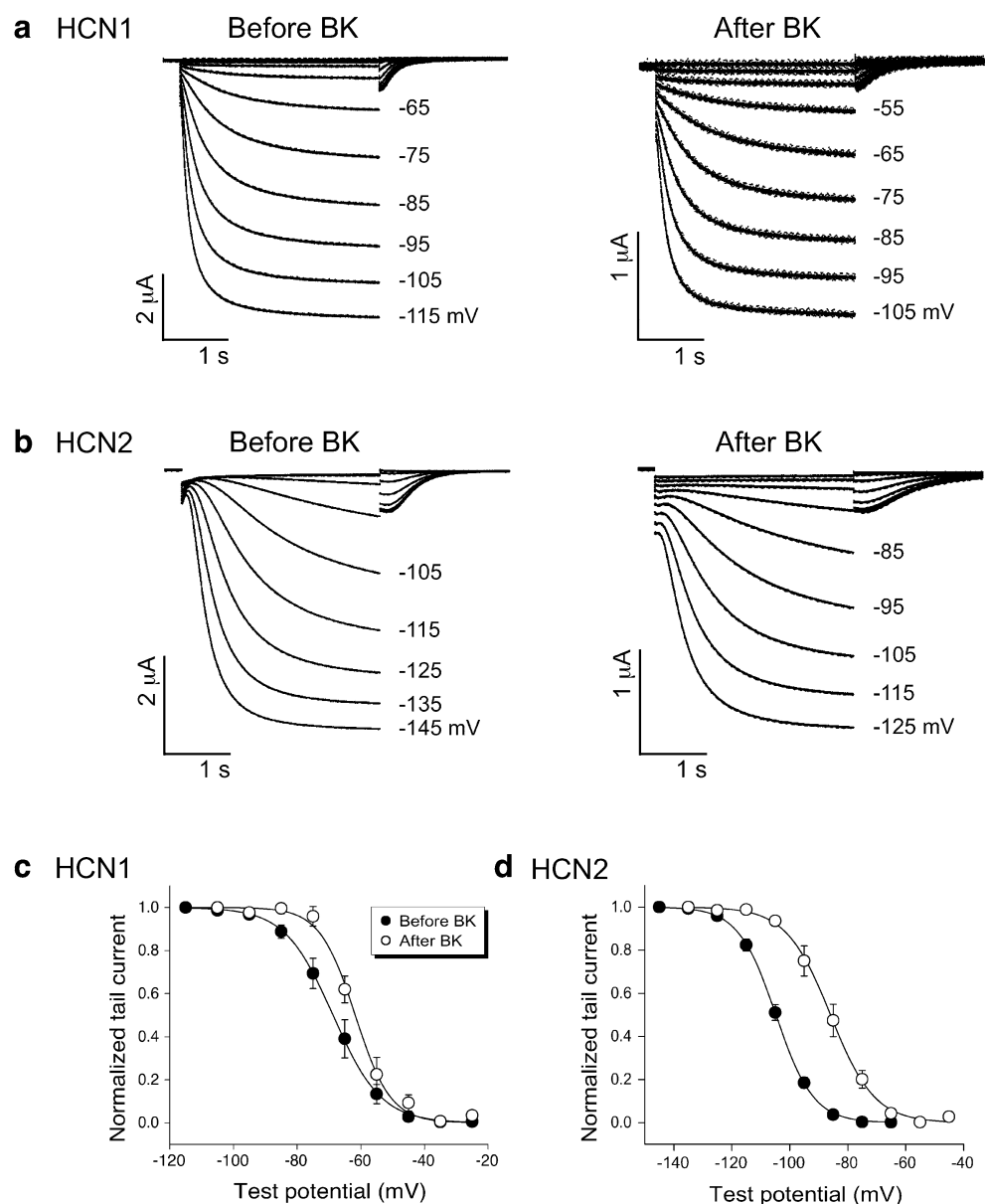
modulated the two HCN isoforms in a qualitatively similar but quantitatively distinct manner. Moreover, the effects on voltage-gating were the opposite of those expected for a decrease in levels of PI(4,5)P$_2$.

Because cAMP directly facilitates the opening of HCN1 and HCN2, we examined whether the paradoxical effect of bradykinin on the voltage-dependence of activation was caused by an increase in the levels of cyclic nucleotides using an HCN2 point mutant, HCN2$_{R591E}$. This mutation of a conserved arginine in the cyclic nucleotide-binding domain prevents binding of cAMP, but does not alter the intrinsic voltage-dependent gating of the HCN2 channel [11]. Bradykinin modulated the gating of HCN2$_{R591E}$ in a manner that was similar to its effects on wild-type HCN2 (Fig. 3). Thus, the peptide produced a depolarizing shift in voltage gating (Figs. 3b and 4a) similar to that seen with

wild-type HCN2 ($\Delta V_{1/2}$ for HCN2$_{R591E}$ was +15.5± 0.7 mV, *n*=12, after ~30 min of BK application). BK application exerted a biphasic effect on the HCN2$_{R591E}$ maximal tail current amplitude, with an early increase followed by a decrease to less than 50% of the initial tail current amplitude before receptor activation, similar to the effects of BK on wild-type HCN2 (Fig. 4b).

Bradykinin also produced a twofold slowing of the time course of tail current deactivation of the mutant channel during steps to −40 mV (Fig. 4d; Table 1; see also Fig. 9c), again similar to its action on wild-type HCN2. The only difference between the effects of bradykinin on HCN2$_{R591E}$ compared to wild-type HCN2 was a somewhat more marked speeding in the rate of activation of the mutant channel (Fig. 4c; see also Fig. 9b). The effects of bradykinin to speed the kinetics of channel activation were
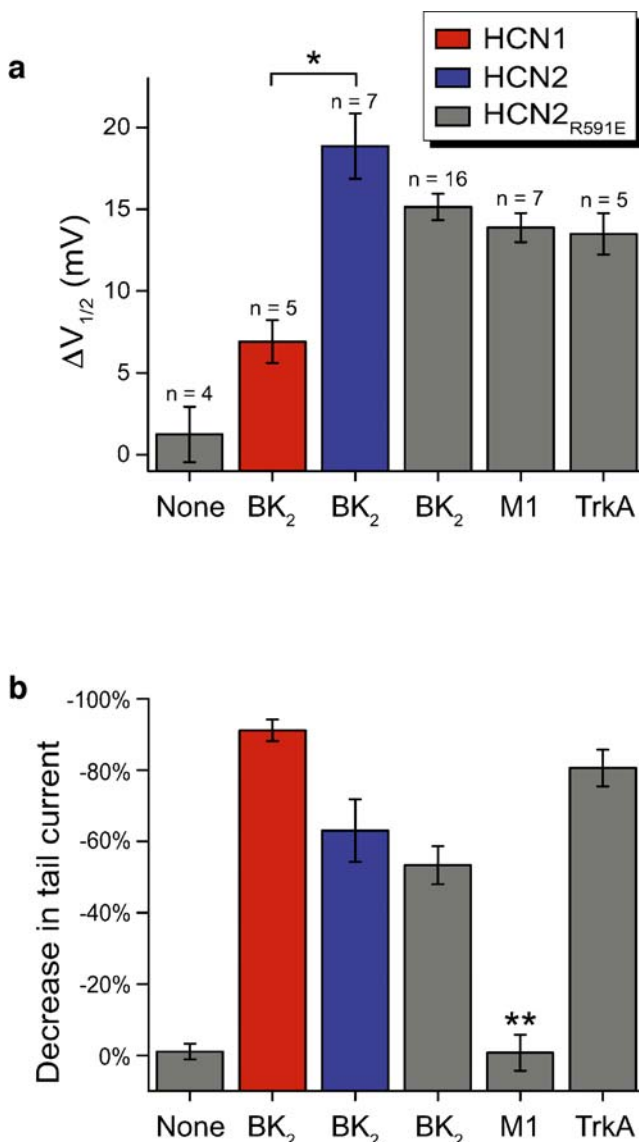
Fig. 2 Modulation of wild-type and mutant HCN channels by cell surface receptors coupled to phospholipase C. Oocytes expressing HCN channel and cell surface receptor pairs were exposed to receptor agonist for 28.5 min, resulting in changes in HCN channel $V_{1/2}$ (**a**) and maximal tail current amplitude (**b**). Channel-receptor pairs, from *left* to *right*: HCN2$_{R591E}$ (*gray*) without addition of agonist (*none*), wild-type HCN1 (*red*) and BK$_2$, wild-type HCN2 (*blue*) and BK$_2$, HCN2$_{R591E}$ and BK$_2$, HCN2$_{R591E}$ and muscarinic M1 receptor, and HCN2$_{R591E}$ and TrkA. The difference between the shift in V$_{1/2}$ of HCN1 and that in HCN2 after BK$_2$ receptor activation was statistically significant (*$P<0.001$; ANOVA; post hoc). The differences between the decrease in HCN2$_{R591E}$ tail current in response to M1 receptor activation and the decreases in tail current for all other channel–receptor pairs (except for HCN2$_{R591E}$ without addition of agonist) were also statistically significant (**$P<0.001$; ANOVA, post hoc). *Error bars* indicate SEM. Number of experiments are shown above each bar

rapid, occurring within 90 s of peptide application (Fig. 4c). In contrast, the slowing of channel deactivation kinetics occurred over a much slower time course, similar to the time course of the shift in $V_{1/2}$ (Fig. 4d). The overall

similarity in the actions of bradykinin on the voltage-dependence of activation, maximal tail current amplitude, and kinetics of deactivation for wild-type HCN2 vs the HCN2$_{R591E}$ mutant indicates that these effects were not mediated by the direct modulatory actions of cAMP on HCN2 function.

In some cell types, receptor-mediated decreases in total PI(4,5)P$_2$ concentration are transient, with basal PI(4,5)P$_2$ levels restored in as little as 30 s during maintained receptor stimulation [58]. To determine whether there was an early hyperpolarizing shift in HCN channel gating, reflecting a transient decrease in PI(4,5)P$_2$ levels, we examined the time course of BK action on HCN2$_{R591E}$ using a more rapid voltage pulse protocol. Because measurements of HCN currents at such early times were complicated by the large transient $I_{Cl,Ca}$, we preincubated oocytes in 50 μM 1,2-bis (o-aminophenoxy)ethane-N,N,N,N-tetraacetic acid tetra (acetoxymethyl) ester (BAPTA-AM) for 2 h to chelate intracellular calcium. (As will be shown below, this does not alter the regulation of I_h by BK).

After determining a full activation curve for HCN2$_{R591E}$ in the BAPTA-loaded oocytes, we switched to a voltage protocol that permitted the rapid assessment of changes in the voltage-dependence of I_h gating and maximal tail current amplitude. The membrane was held at −40 mV and pairs of hyperpolarizing test pulses (3 s) were applied, which alternately stepped the membrane potential to either the initial $V_{1/2}$ for activating HCN2$_{R591E}$ (−88 to −99 mV) or to −135 mV, a voltage that maximally activated the channels (Fig. 5a). The ratio of the tail current amplitude after a step to the initial $V_{1/2}$ to the tail current amplitude following a step to −135 mV provided a sensitive assay for shifts in the voltage-dependence of gating.

In the five oocytes tested in this manner, we failed to detect any early hyperpolarizing shift in channel activation. Rather, BK increased the fractional activation of channels at the initial $V_{1/2}$ within 15 s (see Fig. 5b for a representative example), indicating a rapid depolarizing shift in activation. The magnitude of the voltage shift then slowly increased over the next 15–30 min during continuous exposure to BK. Thus, even at early times, the effects of bradykinin on HCN2 were the opposite of those expected for a decrease in PI(4,5)P$_2$ levels.

Dependence of HCN channel modulation on PLC activity

The unexpected depolarizing shift in HCN gating with BK raised the question as to whether its effects were, in fact, mediated by PLC activation. To test this possibility, we first examined whether other PLC-coupled receptors produced a similar depolarizing shift in HCN channel activation. HCN2$_{R591E}$ was therefore coexpressed with either the M1 muscarinic ACh receptor, which, like BK$_2$ is coupled to G$_{q/11}$

Table 1 Normalized time constants of deactivation after receptor activation

HCN channel	Activated receptor	Drug treatment	Normalized time constant of deactivation (mean±SEM)	n
HCN2$_{R591E}$	N/A	N/A	1.00±0.09	4
HCN1	BK$_2$	N/A	1.60±0.16	5
HCN2	BK$_2$	N/A	2.12±0.14*	7
HCN2$_{R591E}$	BK$_2$	N/A	2.13±0.08*	16
HCN2$_{R591E}$	M1	N/A	1.98±0.11*	7
HCN2$_{R591E}$	TrkA	N/A	1.60±0.06	5
HCN2$_{R591E}$	BK$_2$	DMSO, 0.1%	1.68±0.08	12
		U73122, 10 μM	0.99±0.18**	4
		U73343, 10 μM	1.74±0.13	4
HCN2	(I.O. Patch)	DMSO, 0.1%	1.23±0.13	3
		SAG, 50 μM	1.06±0.10	6
		N/A	1.12±0.04	3
		IP$_3$, 50 μM	1.11±0.06	5
HCN2$_{R591E}$	BK$_2$	DMSO, 0.153%	1.73±0.04	4
		BAPTA-AM, 50 μM	1.49±0.16	4
		DMSO, 0.1%	1.84±0.19	5
		Staurosporine, 1 μM	1.59±0.07	5
		Calphostin C, 3 μM	1.63±0.12	5
		RO 31-8425, 3 μM	1.52±0.04	5
		DMSO, 0.2%	2.07±0.19	4
		R59949, 10 μM	2.20±0.46	4
		DMSO, 0.1%	2.06±0.14	10
		Wortmannin, 100 nM	2.06±0.11	4
		Wortmannin, 300 nM	1.88±0.10	5
		Wortmannin, 500 nM	1.34±0.16	4
		Wortmannin, 1 μM	1.22±0.26	4

Effects of various agents on time constants of tail current deactivation. Oocytes expressing the indicated HCN channel and receptor were pretreated with the indicated drug. Subsequently, the time constants of deactivation at −40 mV were assessed in whole oocytes immediately before and 28.5 min after receptor activation. The values before receptor activation were divided by the values after receptor activation to determine the normalized time constants of deactivation. In experiments using inside–out patches from oocytes expressing HCN2 (I.O. patch group) time constants of deactivation were assessed before and after 22.5 min of bath application of the indicated drugs. Numbers of oocytes or patches are indicated (n). BK$_2$ receptor activation resulted in statistically significant slowing of deactivation for HCN2 and HCN2$_{R591E}$; M1 receptor activation resulted in statistically significant slowing of HCN2$_{R591E}$ (*; $P<0.002$; ANOVA, Post Hoc). U73122 treatment blocked the effect of BK$_2$ receptor activation to slow deactivation of HCN2$_{R591E}$ when compared to treatment with both 0.1% DMSO and U73343 (**$P<0.01$; ANOVA, Post Hoc). There were no statistically significant differences among the normalized time constants of deactivation for oocytes treated with staurosporine, calphostin C, RO 31-8425, and DMSO ($P>0.31$; ANOVA).

and PLCβ, or the receptor for nerve growth factor, TrkA, which is coupled to PLCγ. Activation of either the M1 or TrkA receptor produced a positive shift in activation gating and a slowing of deactivation kinetics of HCN2$_{R591E}$, similar to the effects of BK (Fig. 2a and Table 1). However, whereas TrkA also decreased the maximal tail current amplitude, similar to the effects of BK, activation of the M1 cholinergic receptor did not alter tail current amplitude (Fig. 2b).

Thus, three different receptors coupled to PLC activation all produced a depolarizing shift in HCN2 gating and a slowing of channel deactivation. However, the receptors differed in their ability to decrease maximal tail current amplitude.

To determine the dependence of HCN channel modulation on PLC more directly, we examined the effects of the PLCβ inhibitor U73122 on the response to bradykinin. Oocytes were incubated for 20 min before receptor activation in 10 μM U73122, 10 μM U73343 (an inactive analog), or 0.1% DMSO, the vehicle for U73122 and U73343 [70]. U73122 specifically inhibited the depolarizing shift in $V_{1/2}$ (Fig. 6a$_1$) and the slowing of deactivation in response to BK (Table 1). However, the PLC antagonist did not alter the effects of BK to suppress tail current amplitude (Fig. 6a$_2$). BK$_2$ receptor activation therefore results in a PLCβ-dependent shift in the voltage dependence of HCN channel gating to more positive potentials. However, the

Fig. 3 BK$_2$ receptor activation alters HCN2$_{R591E}$ gating and current. **a** Macroscopic HCN2$_{R591E}$ currents shown for an oocyte in response to a series of hyperpolarizing voltage steps before (*left*) and after (*right*) 28.5 min of incubation in bradykinin. **b** Mean normalized tail currents from HCN2$_{R591E}$ (n= 16) plotted as a function of test potential and fit with the Boltzmann equation. Data obtained before (*filled circles*) or after (*open circles*) bradykinin exposure. *Error bars* to indicate SEM are smaller than the symbols
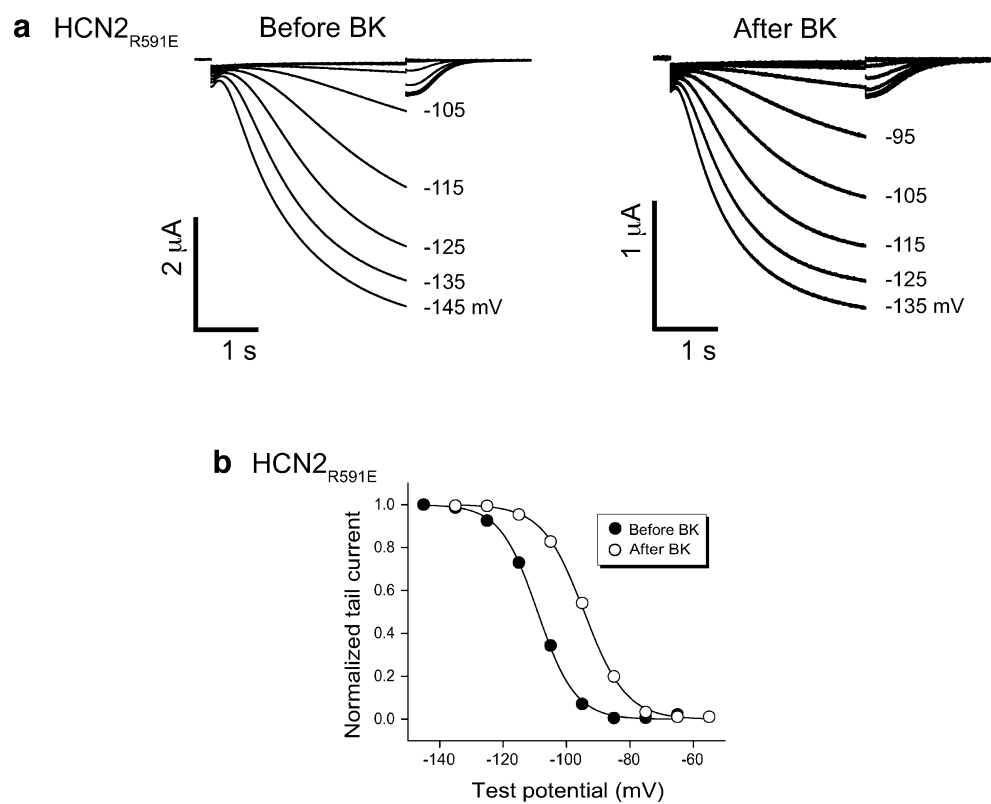

effect of BK to suppress current amplitude appears to occur through a PLCβ-independent path.

To investigate the role of PLCγ in the modulation of HCN2 by the TrkA receptor, we examined two mutants of

the receptor. The TrkA Y499F mutant is deficient in signaling through the MAPK and PI 3-kinase/AKT downstream pathways, whose activation requires phosphorylation of Y499 to recruit Shc and FRS-2 [44, 78]. In contrast,

Fig. 4 Time course of the effect of BK$_2$ receptor activation on HCN2$_{R591E}$ channels. The depolarizing shift in $V_{1/2}$ ($\Delta V_{1/2}$, **a**), normalized tail current (**b**), time constant (τ) of activation at −135 mV (**c**), and time constant of deactivation at −40 mV (**d**) of HCN2$_{R591E}$ channels plotted as a function of time after addition of bradykinin to the bath solution (n=16). *Error bars* show SEM
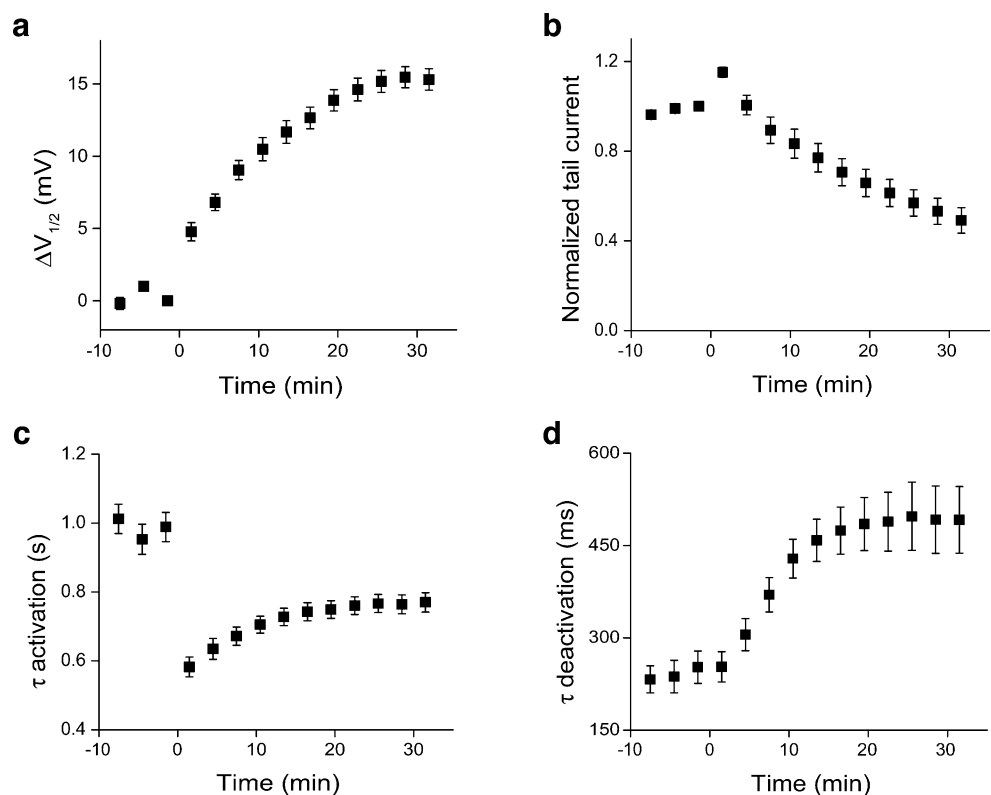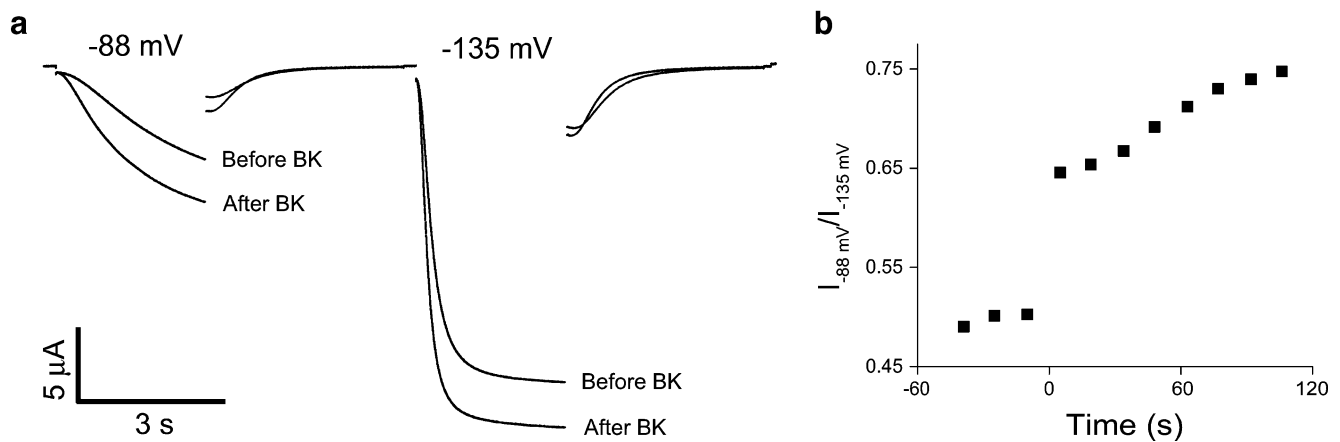
Fig. 5 BK_2 receptor activation causes an immediate depolarizing shift in the $V_{1/2}$ of $HCN2_{R591E}$. To eliminate the Ca^{2+}-activated Cl^- current, oocytes expressing $HCN2_{R591E}$ and BK_2 were incubated in 50 μM BAPTA-AM before recording. Every 14 s, oocyte membrane potential was stepped from a holding potential of −30 mV to two test potentials, one near the $V_{1/2}$ of $HCN2_{R591E}$ before receptor activation (−88 mV) and the other at a hyperpolarized voltage that ensures maximal channel activation (−135 mV). Tail currents were recorded upon return of membrane potential to −40 mV. **a** Macroscopic $HCN2_{R591E}$ currents shown for an individual whole oocyte immediately before and after BK_2 receptor activation. **b** Peak tail current amplitude after a hyperpolarizing step to −88 mV normalized by peak tail current amplitude after a step to −135 mV as a function of time before and during application of bradykinin. Tail currents were measured at −30 mV
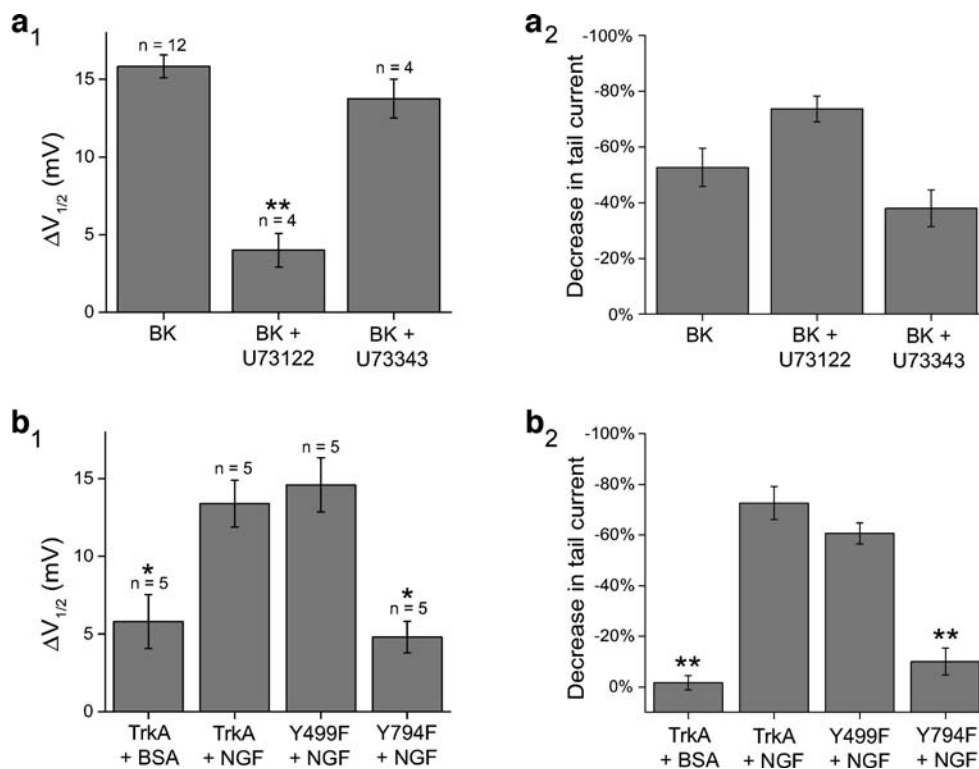
Fig. 6 Dependence of receptor-mediated modulation of $HCN2_{R591E}$ on phospholipase C activity. a_1 and a_2 The effect of 28.5 min exposure to bradykinin on $V_{1/2}$ (a_1) and maximal tail current amplitude (a_2) in the presence of 10 μM U73122 (BK+U73122), a PLC inhibitor; 10 μM U73343 (BK+U73343), an inactive analog; or 0.1% DMSO (BK), the vehicle for U73122 and U73343. The differences between the $\Delta V_{1/2}$ in response to BK in the presence of U73122 and the $\Delta V_{1/2}$ in response to BK in DMSO alone or U73343 were statistically significant (**$P<0.001$; ANOVA, post hoc). b_1 and b_2 The effects of 28.5 min exposure to NGF or BSA (vehicle for NGF) on the $V_{1/2}$ (b_1) and maximal tail current amplitude (b_2) for oocytes expressing wild-type TrkA (TrkA + BSA or TrkA + NGF), the Y499F TrkA mutant (Y499F+NGF), or the Y794F mutant (Y794F + NGF). The four conditions fell into two groups: I. TrkA+BSA and Y794F+NGF; II. TrkA+NGF and Y499F+NGF. The differences in $\Delta V_{1/2}$ or maximal tail current between each member of group I and each member of group II were statistically significant; $P<0.02$ for $\Delta V_{1/2}$ (*) and $P<0.001$ for tail current (**); ANOVA, post hoc. *Error bars* indicate SEM

the TrkA Y794F mutant is deficient in PLC signaling, which depends on the binding of PLCγ to phosphorylated Y794 [39]. Activation of the Y499F TrkA mutant with nerve growth factor produced a normal-sized shift in $V_{1/2}$ and decrease in maximal tail current amplitude (Fig. 6b$_1$, b$_2$). In contrast, both the shift in $V_{1/2}$ and decrease in tail current were almost completely eliminated in the Y794F PLC-signaling mutant. Thus, the TrkA-mediated shift in HCN gating and suppression of tail current appear to depend on PLCγ.

Classical downstream effectors of PLC do not mediate BK$_2$ receptor modulation of HCN2$_{R591E}$

To further investigate the mechanism of HCN channel modulation, we next examined the effects of the two molecules produced by PLC-mediated hydrolysis of PI(4,5)P$_2$: IP$_3$ and DAG. Direct application of either IP$_3$ or an analog of DAG, 1-stearoyl-2-arachidonoyl-sn-glycerol (SAG), to patches excised from oocytes expressing HCN2$_{R591E}$ had no effect on channel function. Thus, after >20 min of application of 50 μM SAG, the $V_{1/2}$ (Fig. 7a$_1$; $P>0.47$; ANOVA), time constant of deactivation (Table 1; $P>0.52$; ANOVA), and tail current amplitude (Fig. 7a$_2$; $P>0.75$; ANOVA) showed no statistically significant difference from control values. A similar period of exposure to 50 μM IP$_3$ also failed to alter the $V_{1/2}$ (Fig. 7a$_1$; $P>0.24$; ANOVA), time constant of deactivation (Table 1; $P>0.43$; ANOVA), or tail current amplitude (Fig. 7a$_2$; $P>0.42$; ANOVA). Thus, the receptor-

dependent modulation of HCN2 studied in this paper does not involve direct channel regulation by IP$_3$ or DAG.

Might the modulatory effects of receptor activation on HCN2 channel function result from the IP$_3$-dependent rise in intracellular Ca^{2+} levels? To test this idea, oocytes were preincubated in 50 μM BAPTA-AM for 2 h to chelate intracellular Ca^{2+}. Although BAPTA-AM treatment inhibited the ability of BK to activate the endogenous Ca^{2+}-activated Cl$^-$ current present in the oocytes, it failed to alter the modulatory effects of BK on HCN2$_{R591E}$ (Fig. 7b, Table 1), including the shift in voltage-dependent gating ($P>0.3$), slowing in the rate of deactivation ($P>0.09$) or suppression of maximal tail current amplitude ($P>0.4$).

Finally, we investigated the involvement of protein kinases and C$_1$ domain-containing proteins. A 2-h preincubation of oocytes with the broad-spectrum kinase inhibitor staurosporine, the C$_1$ domain inhibitor calphostin C, or the protein kinase C inhibitor RO 31-8425, had no effect on the ability of BK to modulate HCN2$_{R591E}$. Thus, application of BK produced a normal shift in $V_{1/2}$ (Fig. 8a$_1$), slowing in the time course of deactivation (Table 1), and inhibition in maximal tail current amplitude (Fig. 8a$_2$). We verified that the inhibitors did indeed block PKC activity by their ability to antagonize the PKC-dependent effect of phorbol esters to increase the magnitude of the P/Q-type Ca^{2+} current upon expression of Ca$_V$2.1 in the oocytes [42].

As an independent test of the role of DAG and its downstream effectors in the modulatory actions of BK, we

Fig. 7 The effects of bradykinin on $V_{1/2}$ and tail current for HCN2$_{R591E}$ are not mediated by classical signaling pathways downstream of phospholipase C. a$_1$ and a2 Changes in the midpoint voltage of activation ($\Delta V_{1/2}$, a$_1$) and tail current (a$_2$) after 22.5 min of bath application of 0, 10, and 50 μM 1-stearoyl-2-arachidonyl-sn-glycerol (SAG) and of 0 and 50 μM inositol trisphosphate (IP$_3$) to HCN2$_{R591E}$ channels in inside-out macropatches. b$_1$, b$_2$, and b$_3$ Effects of 2 h preincubation of oocytes in 50 μM BAPTA-AM or 0.153% DMSO (control; the vehicle for BAPTA-AM) on the response to BK: b$_1$ and b$_2$ show effect of BK to shift $V_{1/2}$ and decrease tail current for HCN2$_{R591E}$, respectively. b$_3$ shows effect of BK to activate the endogenous Ca^{2+}-activated Cl$^-$ current. Error bars indicate SEM
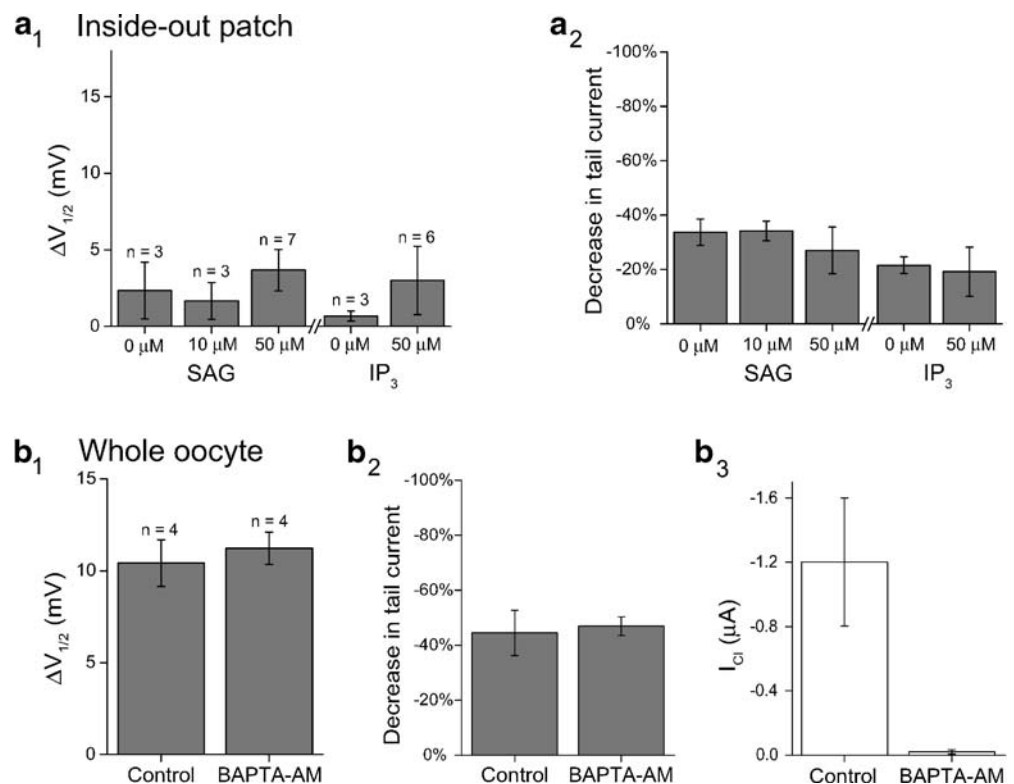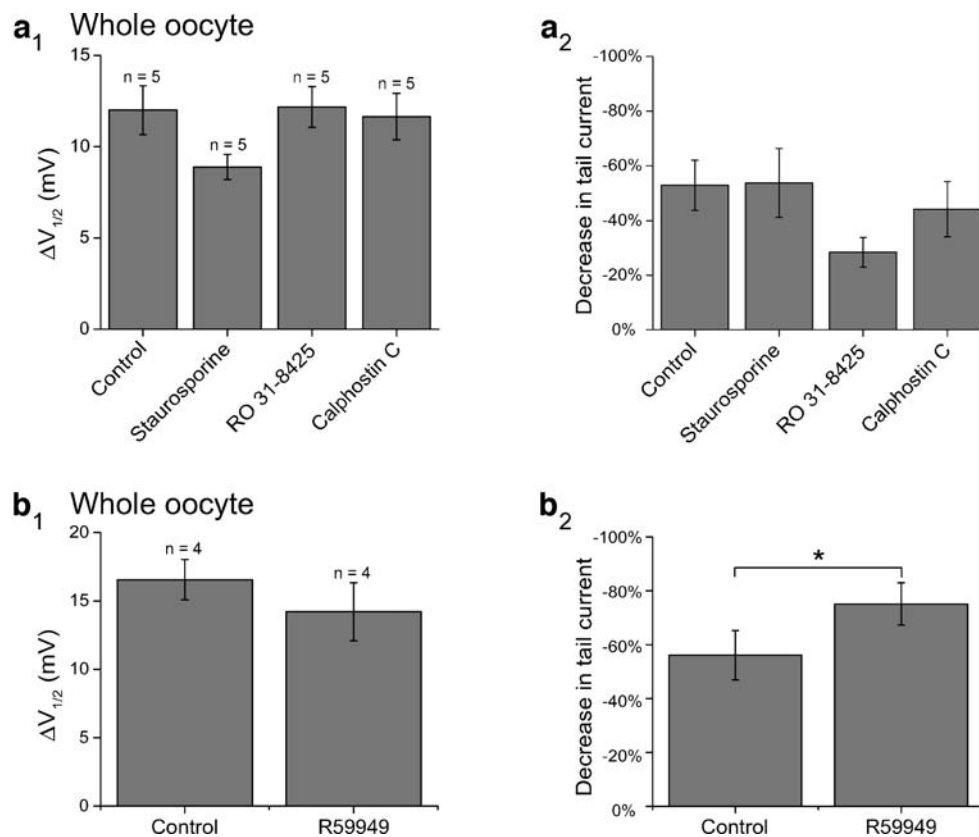
Fig. 8 The effects of bradykinin on $V_{1/2}$ and tail current for HCN2$_{R591E}$ are not mediated by classical signaling pathways downstream of phospholipase C. a_1 and a_2 Effects of inhibitors of PKC and C1 domain-containing proteins on response to BK. Oocytes were preincubated for 2 h in 1 μM staurosporine, 3 μM Ro-31-8425, 3 μM calphostin C, or 0.1% DMSO (control), the vehicle for all three compounds. The effects of BK$_2$ receptor activation on $V_{1/2}$ (a_1) and tail current amplitude (a_2) for HCN2$_{R591E}$ are shown under the various incubation conditions. No statistically significant differences in $\Delta V_{1/2}$ ($P>0.17$; ANOVA) or tail current amplitude were observed ($P>0.25$; ANOVA). b_1 and b_2 Effects of DAG kinase inhibitor R59949 on response to BK: Oocytes were incubated for 2 h in 10 μM R59949 or 0.2% DMSO (control), the vehicle for R59949. The effects of BK$_2$ receptor activation on $V_{1/2}$ (b_1) and tail current amplitude (b_2) for HCN2$_{R591E}$ are shown under the two conditions. The BK-induced decrease in tail current was significantly greater in the presence of R59949 (*$P<0.05$; t test). *Error bars* indicate SEM

examined the effects of inhibitors of DAG kinase, the enzyme that converts DAG to phosphatidic acid. Recently, the DAG kinase inhibitor R59949 was shown to inhibit the effect of phorbol esters to cause a positive shift in the gating of HCN channels expressed in oocytes [17], implicating phosphatidic acid in this effect. In contrast, if DAG itself were an important mediator of the action of BK, then inhibition of DAG kinase should potentiate the effects of BK by increasing the free concentration of DAG. However, we found that preincubation of oocytes for 2 h in 10 μM R59949 had little or no effect on the action of BK to shift the voltage dependence or slow the kinetics of deactivation of HCN2$_{R591E}$ channels. Thus, in the presence of R59949, BK produced a 14.2±2.1 mV depolarizing shift and a 2.20±0.46 fold increase in the time constant of deactivation (Fig. 8b$_1$ and Table 1), similar to the response to BK after preincubation in vehicle alone (0.2% DMSO; Fig. 8b$_1$ and Table 1; 16.6±1.5 mV depolarizing shift in $V_{1/2}$, $P>0.26$; 2.07±0.19 fold increase in the time constant of deactivation, $P>0.40$).

Interestingly, the DAG kinase inhibitor did enhance the magnitude of the inhibitory effect of BK on tail current amplitude (Fig. 8b$_2$). Thus, in the presence of R59949, BK caused a 74.8±7.8% reduction in current amplitude ($n=4$), which is significantly greater than the 56.1±9.2% reduction in current amplitude produced by BK when applied in the presence of DMSO ($P<0.05$; t test). Thus, DAG-activated proteins, including PKC and DAGK, appear unlikely to be involved in the PLC-dependent modulation of either the voltage-dependence or rate of deactivation of HCN channel gating, although the effect of BK to decrease tail current amplitude may depend on DAG production.

PI kinase inhibitors block the shift in HCN voltage gating but do not alter the decrease in maximal current in response to BK

The PLC-dependent effects of BK, ACh, and NGF to cause a depolarizing shift in gating and slow deactivation of

HCN2 channels resemble the direct effects of $PI(4,5)P_2$ on HCN2 channel gating [51, 92]. Given that $PI(4,5)P_2$ synthesis can be enhanced after activation of PLC [28, 35], including in response to bradykinin [19, 29], we next explored the hypothesis that the modulatory actions on HCN2 channel function of receptor-mediated activation of PLC are caused by an *increase* in local $PI(4,5)P_2$ levels because of an enhancement in $PI(4,5)P_2$ synthesis. To test this idea, we inhibited $PI(4,5)P_2$ synthesis by blocking the activity of PI kinases using wortmannin or LY294002 [3, 76]. Although these agents exhibit some selectivity for inhibiting PI 3-kinases, at higher concentrations they also block the activity of PI 4-kinases, which are required for the synthesis of $PI(4,5)P_2$. Thus, whereas wortmannin inhibits PI 3-kinase at nanomolar concentrations ($IC_{50} \approx 1$–4 nM), it

also inhibits PI 4-kinases at ~100–1,000-fold higher concentrations [1, 3, 45, 48]. Similarly, in membrane patches from *Xenopus* oocytes, LY294002 maximally inhibits PI 3-kinase at a concentration of 10 μM, but will also block PI 4-kinase when applied at higher concentrations ($IC_{50} \approx 50$–100 μM) [3, 64].

After a 2-h incubation in 1 μM wortmannin (a concentration that blocks PI 4-kinases) or vehicle alone (0.1% DMSO), oocytes coexpressing $HCN2_{R591E}$ and the BK_2 receptor were exposed to bradykinin. Pretreatment with wortmannin produced a marked inhibition in the ability of bradykinin to cause a depolarizing shift in the $V_{1/2}$ (Figs. 9a and 10a). Thus, in the presence of 1 μM wortmannin, bradykinin shifted the $V_{1/2}$ by only $+2.6 \pm 2.3$ mV, compared to the $+15.4 \pm 0.8$ mV shift seen when

Fig. 9 Effects of the PI kinase inhibitor wortmannin on the actions of bradykinin to modulate $HCN2_{R591E}$ currents. Oocytes were incubated in 1 μM wortmannin (*right*; *n*=4) or 0.1% DMSO, the vehicle for wortmannin (*left*; *n*=4), for 2 h before recording. **a** Mean tail current activation curves obtained before (*filled circles*) and after (*open circles*) a ~30-min incubation in 100 nM bradykinin. **b** Mean time constants of activation during hyperpolarizing steps to −125, −115, and −105 mV, before or after (+ BK) incubation in bradykinin in presence of DMSO alone (*left panel*) or DMSO plus wortmannin (*right panel*). **c** Mean time constants of tail current deactivation during steps to −40 mV, before or after (+ Bk) incubation in bradykinin in presence of DMSO alone (*left panel*) or DMSO plus wortmannin (*right panel*). **P<0.05* vs control (*t* test)
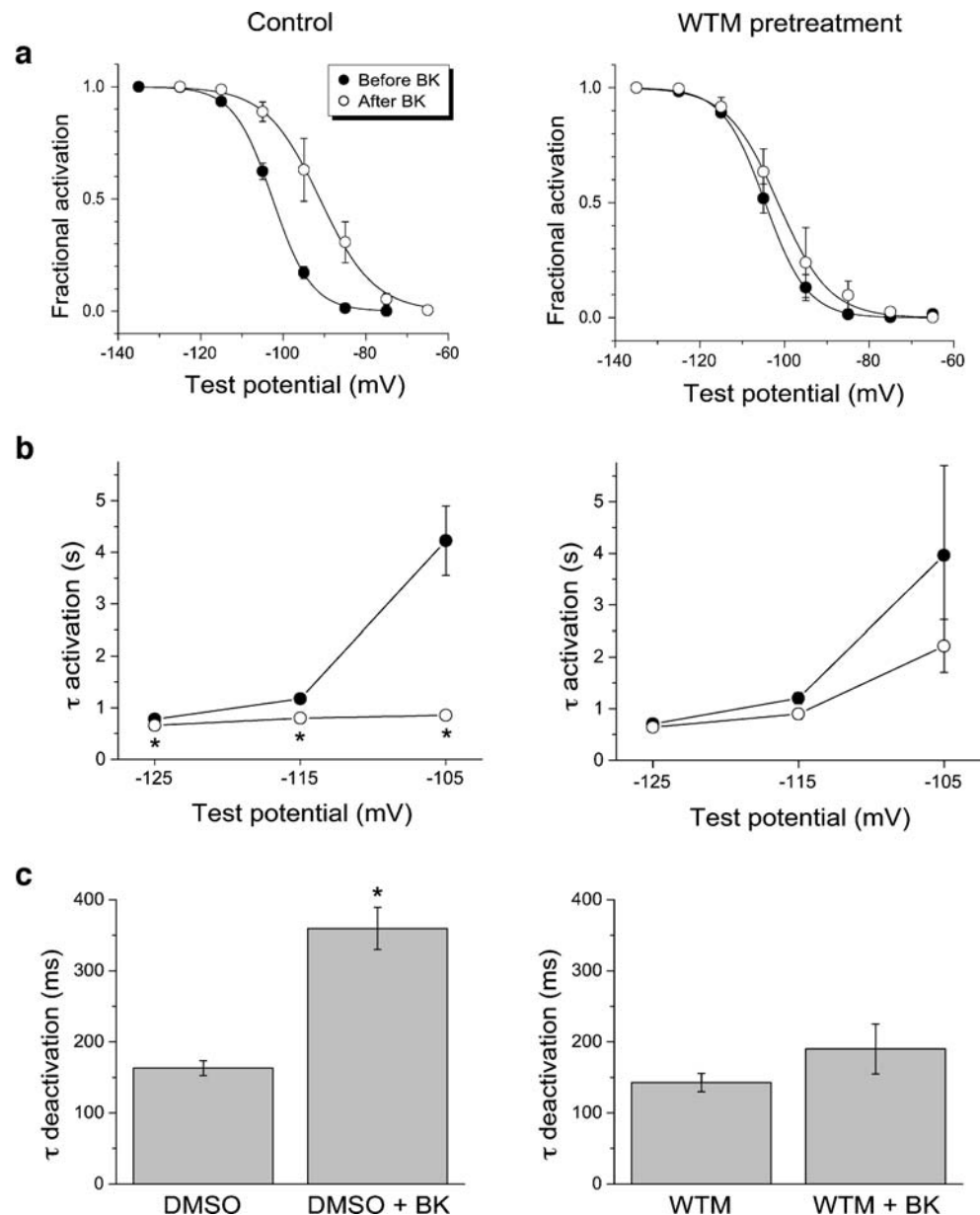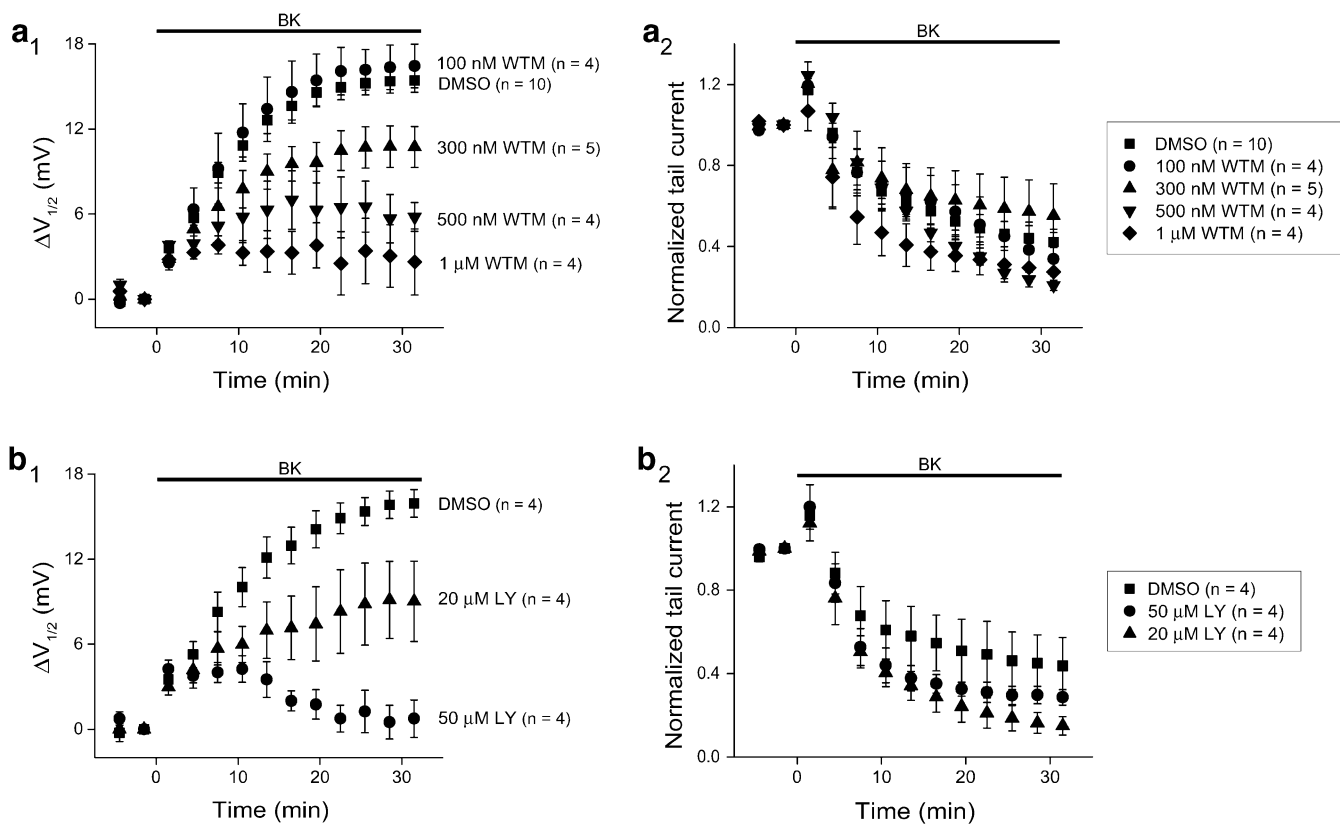
Fig. 10 Dose–response curves for the actions of the PI kinase inhibitors wortmannin and LY294002 on the effects of bradykinin to modulate $HCN2_{R591E}$ function. Before recordings, oocytes expressing $HCN2_{R591E}$ and BK_2 were incubated in a range of wortmannin (WTM, $\mathbf{a_1}$ and $\mathbf{a_2}$) and LY294002 (LY, $\mathbf{b_1}$ and $\mathbf{b_2}$) concentrations or in 0.1% DMSO, the vehicle for the inhibitors. Time course of the effects of BK_2 receptor activation to shift the $V_{1/2}$ ($\mathbf{a_1}$ and $\mathbf{b_1}$) and inhibit maximal tail current amplitude ($\mathbf{a_2}$ and $\mathbf{b_2}$) are shown. *Error bars* indicate SEM

bradykinin was applied in the presence of DMSO ($P< 0.0003$; ANOVA, Post hoc). Wortmannin also blocked the effect of bradykinin to increase the time constant of deactivation (Table 1 and Fig. 9c; $P<0.03$; ANOVA, Post hoc). In contrast, wortmannin only partially blocked the effect of bradykinin to speed the kinetics of channel activation (Fig. 9b) and had no effect on the ability of bradykinin to suppress the maximal tail current amplitude (Fig. 10a_2).

Although the inhibitory effects of wortmannin are consistent with the idea that bradykinin shifts voltage gating by stimulating $PI(4,5)P_2$ synthesis, the inhibition of PI kinases could, in principle, deplete resting levels of $PI(4,5)P_2$, which would prevent the synthesis of any downstream metabolites of $PI(4,5)P_2$ after PLC activation. In fact, preincubation with higher concentrations of wortmannin (≥ 10 μM) did cause hyperpolarizing shifts of the basal $V_{1/2}$ values of recombinant HCN2 in *Xenopus* oocytes [51] and native I_h in dopaminergic neurons [92], consistent with a decrease in resting $PI(4,5)P_2$ levels. However, under the conditions of our experiments, 1 μM wortmannin had no effect on the basal $V_{1/2}$ of $HCN2_{R591E}$, suggesting there was little change in resting $PI(4,5)P_2$ levels. Thus, the $V_{1/2}$ after treatment with wortmannin (-101.7 ± 0.7 mV; $n=4$) was

equal to the value obtained in the presence of DMSO (-101.7 ± 0.9 mV, $n=10$). Moreover, we found that 1 μM wortmannin produced no change in the amplitude of the Ca^{2+}-activated Cl^- current elicited by bradykinin ($I_{Cl,Ca}$ was equal to -0.73 ± 0.30 μA [$n=4$] in the presence of wortmannin vs -0.75 ± 0.25 μA [$n=5$] in DMSO), indicating the production of a normal amount of IP_3 in the presence of the PI kinase inhibitor.

To gain insight into whether the effects of bradykinin required PI 3-kinase or PI 4-kinase activity, we measured the dose–response relation for the inhibition of the bradykinin response with wortmannin (Fig. 10). A concentration of wortmannin between 300 and 500 nM produced a half-maximal inhibition of the effects of BK to shift the $V_{1/2}$ and increase the time constant of deactivation. This IC_{50} value is 100-fold higher than the value for PI 3-kinase inhibition but similar to the concentration range required to inhibit the type IIIα and β isoforms of PI 4-kinase [3]. Thus, our results suggest that the effects of bradykinin on HCN2 gating may depend on activation of PI 4-kinase, consistent with an increase in synthesis of $PI(4,5)P_2$.

Preincubation of oocytes in 50 μM LY294002 also blocked the effect of bradykinin on the voltage dependence

of $HCN2_{R591E}$ gating (Fig. $10b_1$), but had no effect on the reduction in current amplitude (Fig. $10b_2$). The IC_{50} with LY294002 was ~20 μM, in between previously reported IC_{50} values for the inhibition of PI 3-kinases and PI 4-kinases. Importantly, LY294002, even at 50 μM, did not inhibit the bradykinin-induced increase in $I_{Cl,Ca}$ (LY294002: $I_{Cl,Ca}$=−0.71±0.27 μA, n=4; DMSO: $I_{Cl,Ca}$= −0.75±0.32, n=4; both measured at −30 mV), indicating that the inhibitor did not deplete basal levels of $PI(4,5)P_2$. The finding that wortmannin and LY294002 inhibited the modulatory effects of receptor-dependent actions on HCN2 gating without blocking the agonist-induced suppression of maximal current adds further support to the idea that these effects represent two distinct and mechanistically separable actions.

BK_2 receptor modulation of HCN gating is not mediated by tyrosine kinases

Inhibition of tyrosine kinases reduces I_h current amplitude in sinoatrial node myocytes and in *Xenopus* oocytes [81, 85]. To test whether a reduction in tyrosine kinase activity after BK_2 receptor activation might underlie the decrease in maximal current, we treated oocytes expressing $HCN2_{R591E}$ with 2,5-dihydroxymethylcinnamate (200 μM for 20′), an erbstatin analog that inhibits tyrosine kinase activity. Application of BK after a 20′ incubation in this inhibitor produced a normal-sized effect on HCN channel function, with a 16.3±1.8 mV depolarizing shift in $V_{1/2}$, a 1.98±0.20 fold increase in the time constant of deactivation, and a 35.2±10.1% decrease in tail current amplitude. These effects were very similar to the effects of BK under control conditions (20′ incubation in 0.16% DMSO), in which there was a 14.6±0.9 mV depolarizing shift, 1.91±0.09 fold increase in the time constant of deactivation, and a 40.4± 9.4% reduction in tail current amplitude (n=4).

Modulation of I_h in sinoatrial cells by bradykinin

Does the activation of PLC-coupled receptors also lead to a PI kinase-dependent modulation of native HCN channels under more physiological conditions? To examine this question, we tested the effect of bradykinin on endogenous hyperpolarization-activated I_h recorded from sinoatrial myocytes. Because myocyte HCN currents showed prominent rundown during whole-cell recordings, we pretreated populations of myocytes with bradykinin or a control solution and compared the gating properties of I_h from the two populations of cells. Pretreatment of myocytes with 100 nM bradykinin shifted the I_h activation curve to more positive potentials with respect to control cells (Fig. 11a, left). In the absence of bradykinin, the $V_{1/2}$ and slope factor from tail current activation curves were equal to −62.2±

1.6 mV (n=9) and 11.1±0.8 mV, respectively. Bradykinin application produced an ~8-mV positive shift in the $V_{1/2}$ to −54.6±1.7 (n=8), a value significantly different from the control $V_{1/2}$ (P<0.05; t test), with no significant change in slope factor (9.8±0.6 mV, P>0.05).

Importantly, we found that the effect of bradykinin on myocyte HCN channels to shift gating to more positive potentials was largely abolished when the cells were preincubated for 60 min with 10 μM wortmannin (Fig. 11a, right). In the presence of wortmannin alone (no bradykinin), the $V_{1/2}$ was equal to −65.7±2.0 mV (n=8), not significantly different from the value in control myocytes in the absence of wortmannin (−62.2±1.6 mV; P>0.05). However, application of bradykinin in the presence of wortmannin produced only a small, 3-mV shift in the $V_{1/2}$ (to −62.7±1.3 mV; n=8) that was not statistically significant (P>0.05 compared to the $V_{1/2}$ in the absence of bradykinin and presence of wortmannin). There was no change in slope factor, either in response to wortmannin alone (s=9.1±0.8 mV) or with bradykinin in the presence of wortmannin (s=10.5±0.6 mV) (P>0.05).

Our analysis of I_h kinetics (Fig. 11b and c, left) revealed that bradykinin increased the rate of I_h activation during hyperpolarizations and slowed the rate of deactivation during a step to −70 mV. Application of wortmannin blocked the effects of bradykinin on both activation and deactivation kinetics (Fig. 11b, c, right), indicating the role of PI kinase activation. Thus, bradykinin exerted similar PI kinase-dependent effects on the kinetics and steady-state voltage dependence of activation of both recombinant and native HCN currents, although the magnitude of the voltage shift was somewhat smaller in myocytes.

Discussion

Most examples of receptor-dependent regulation of HCN channel activity to date involve changes in levels of intracellular cyclic nucleotides, which directly regulate HCN channel gating. Our present results demonstrate that stimulation of several receptors linked to PLC—the BK_2 bradykinin receptor, the M1 muscarinic ACh receptor, and the TrkA nerve growth factor receptor—regulate the function of recombinant HCN1 and HCN2 channels expressed in *Xenopus* oocytes in a cAMP-independent manner. Activation of these receptors results in a depolarizing shift in the voltage-dependence of HCN activation and a twofold slowing in the rate of channel deactivation. In addition, activation of the BK_2 and TrkA receptors, but not the M1 AChR, inhibits the peak tail current amplitude. The effects of receptor stimulation on the voltage dependence of activation and on deactivation kinetics require the activation of PLC, whereas the inhibitory effects on maximal tail

Fig. 11 Effect of bradykinin on sinoatrial I_h current. **a** *Left*: Mean I_h activation curves obtained in the absence (*filled circles*; n=9) and in the presence (*open circles*; n=8) of 100 nM bradykinin. *Right*: I_h activation curves obtained in the presence of wortmannin (10 μM, *filled circles*; n=8) and in the presence of both wortmannin (10 μM) and bradykinin (100 nM, *open circles*; n=8). **b** Mean activation time constants during steps to −100, −85, and −70 mV. *Left*: values obtained in the absence (*filled circles*) and in the presence (*unfilled circles*) of 100 nM bradykinin. *Right*: values obtained in the presence of wortmannin (10 μM, *filled circles*) and in the presence of both wortmannin (10 μM) and bradykinin (100 nM, *open circles*). **c** Mean time constants of tail current deactivation during steps to −70 mV. *Left*: Time constants obtained in the absence and presence of 100 nM bradykinin. *Right*: values obtained in the presence of wortmannin (10 μM) and in the presence of both wortmannin (10 μM) and bradykinin (100 nM). *P<0.05 vs control (t test)
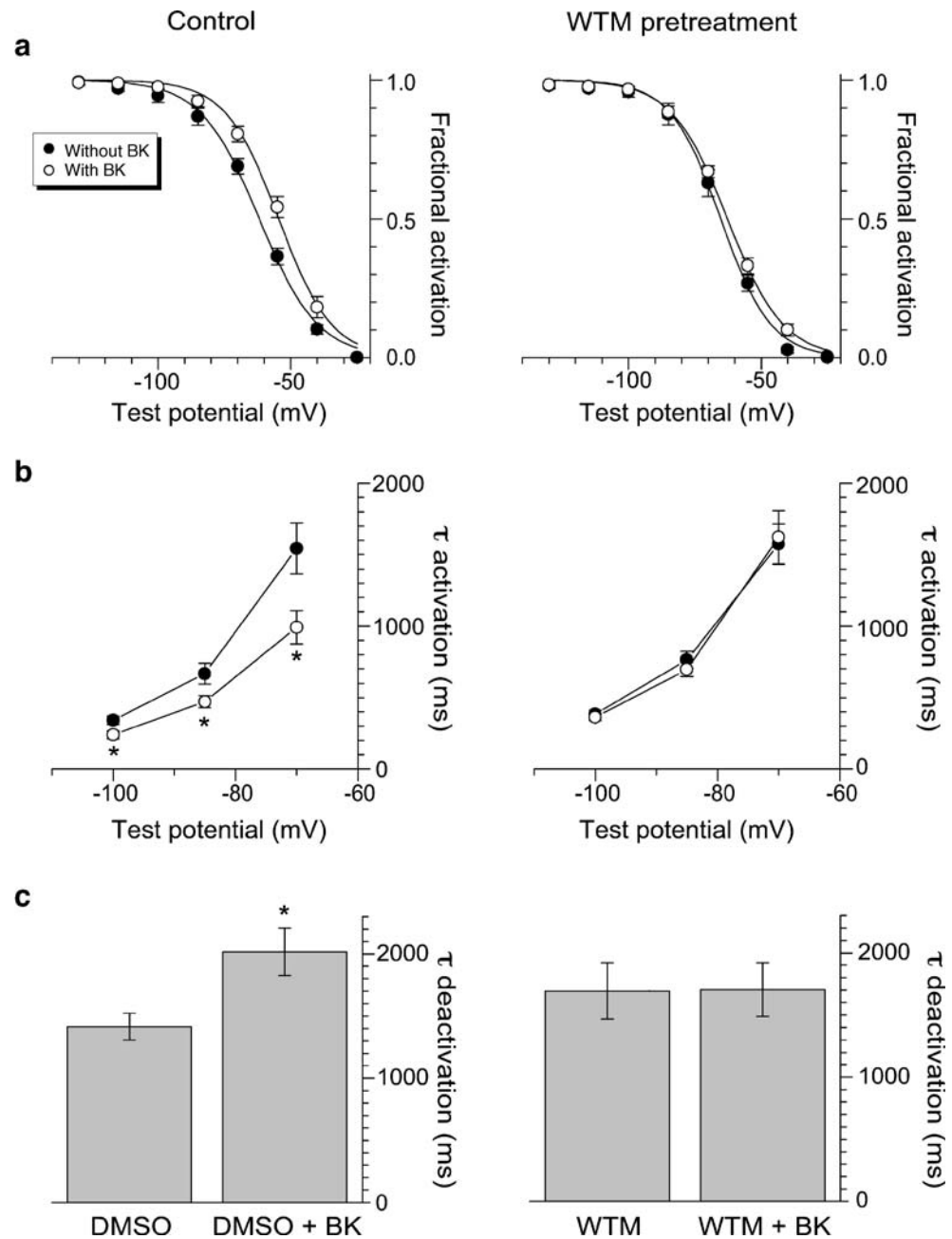
current amplitude are independent of PLC activity. Finally, the PLC-dependent modulatory actions depend on PI kinase activity. The signaling cascade responsible for the PLC-independent decrease in tail current amplitude remains unknown.

Importantly, we find that bradykinin also modulates native hyperpolarization-activated currents in sinoatrial node cells in a manner that resembles the action of this peptide on recombinant HCN1 and HCN2 channels in oocytes, including a positive shift in activation gating and a slowing of the time constant of deactivation. Moreover, these regulatory effects on HCN currents in myocytes also require PI kinase activity. The positive shift in gating with bradykinin is similar in

magnitude to the positive shift seen with cyclic nucleotides, and thus may lead to a significant speeding in cardiac automaticity, as observed with adrenergic agonists. Thus, the mode of HCN channel modulation reported in this paper may represent a novel physiologically relevant mechanism for regulating cellular excitability.

HCN channel modulation by PI(4,5)P$_2$

The positive shift in voltage gating we observed upon activation of three different receptors coupled to PLC activation is opposite to the hyperpolarizing shift in HCN activation expected for a decrease in PI(4,5)P$_2$ levels, based

on the observation that direct application of $PI(4,5)P_2$ to HCN channels in inside-out patches shifts their gating to more positive potentials [51, 92]. This discrepancy is not caused by a difference between intact cells and cell-free patches, as prolonged inhibition of $PI(4,5)P_2$ synthesis with a high concentration of wortmannin *does* cause a hyperpolarizing shift in HCN gating in intact cells [51, 92]. One possible explanation for the contrasting results between PLC stimulation and PI kinase inhibition is that the latter leads to global changes in membrane $PI(4,5)P_2$ levels, whereas receptor-mediated stimulation of PLC activity may produce local decreases in $PI(4,5)P_2$ that are not sensed by the HCN channels. This idea is consistent with the finding that HCN channels may be localized to lipid rafts [4] and caveolae [5], which could contribute to local signaling effects.

It is interesting that the modulation of HCN channels by PLC-linked receptors in *Xenopus* oocytes resembles the alterations in I_h in cardiac sinoatrial node cells after disruption of caveolae with methyl-β-cyclodextrin, which results in a ~10-mV depolarizing shift in gating, a ~twofold increase in the time constant of deactivation, and a small decrease in the time constant of activation [4]. The similarity in effects on HCN channel function may be more than coincidental, as treatment of keratinocytes with methyl-β-cyclodextrin results in the ligand-independent activation of receptor tyrosine kinases coupled to PLCγ [34].

The PLC-linked receptor-dependent actions represent a distinct signaling pathway from previously described mechanisms for regulating HCN channel function

Although an increasing number of regulatory mechanisms that control HCN channel function have been identified, they are unlikely to mediate the modulatory effects of PLC-linked receptors studied in this paper. First, we can rule out alterations in levels of cyclic nucleotide, the canonical HCN channel modulator, as the receptor-mediated changes in channel gating were preserved in the $HCN2_{R591E}$ mutant, which fails to bind cyclic nucleotide. Second, although src tyrosine kinase activity shifts the voltage dependence of HCN gating to positive potentials and speeds the kinetics of channel activation [2, 93], an increase in tyrosine phosphorylation is unlikely to be involved, as staurosporine, an inhibitor of src activity, did not inhibit the receptor-dependent modulation of HCN2. In addition, src does not alter channel deactivation kinetics [2, 93], a prominent component of the receptor-dependent actions we have characterized.

Activation of PKA [10, 73, 84] and PKC [17] can shift the voltage dependence of HCN channel activation to more depolarized potentials and PKC activation also reduces HCN current amplitude [9]. However, neither PKA nor PKC is likely to mediate the effects of receptor stimulation examined in our study, as we found that staurosporine, which blocks both PKA and PKC, and calphostin C and RO 31-8425, which potently inhibit PKC, all failed to affect the receptor-dependent channel modulation. Although a rise in intracellular Ca^{2+} can facilitate HCN channel opening [23, 41], this mechanism can be ruled out as well because we found that preincubation of oocytes with the Ca^{2+} chelator BAPTA-AM had no effect on HCN2 modulation, even though this pretreatment did block the activation of the Ca^{2+}-dependent Cl^- current.

HCN channels have recently been shown to be regulated by p38 MAP kinase activity [52], which produces a constitutive 25-mV depolarizing shift in HCN gating in CA1 pyramidal neurons. Although we have not directly examined the role of this pathway, p38 MAP kinase activity does not slow HCN channel deactivation, a key component of the effects observed in this study after receptor-mediated activation of PLC. Moreover, we failed to detect significant levels of activated p38 MAP kinase in *Xenopus* oocytes, either under resting conditions or upon stimulation with anisomycin, a well-known activator of p38 MAP kinase (J. Dudman, D. Bell, and S.A. Siegelbaum, unpublished results).

Finally, a recent study has demonstrated an interesting and complex regulatory effect of phorbol esters on HCN channel gating [17]. These compounds produce a depolarizing shift in the voltage dependence of HCN channel activation and decrease the maximal HCN channel current, similar to the modulatory effects of the PLC-coupled receptors and of $PI(4,5)P_2$ application. However, the effects of phorbol esters require the activation of PKC and diacylglycerol kinase but are independent of PI kinase activity [17], in contrast to the effects examined in our study.

Role of $PI(4,5)P_2$ synthesis in the modulation of HCN channel function through receptor-dependent stimulation of PLC

Several lines of evidence support the idea that the modulatory effects we observe on HCN channel function in response to receptor-mediated activation of PLC result, at least in part, from an increase in local $PI(4,5)P_2$ levels. First, as discussed above, our data rule out almost all other known modulatory effectors that have been previously demonstrated to regulate HCN channel function. Second, the depolarizing shift in voltage-dependent gating and slowing of deactivation kinetics observed upon receptor activation closely resembles the modulatory actions of exogenous application of $PI(4,5)P_2$ to HCN channels in cell-free inside-out patches [51]. Third, the effects of receptor stimulation were blocked by two inhibitors of PI kinase activity.

A precondition that must be met for a receptor-mediated increase in PI(4,5)P$_2$ levels to be able to shift HCN gating to more positive voltages is that basal levels of PI(4,5)P$_2$ must be insufficient to produce a maximal positive shift in channel gating. Although HCN2 channels are strongly regulated by basal levels of PI(4,5)P$_2$ [51, 92], a quantitative analysis of our results indicates that elevations in the concentration of PI(4,5)P$_2$ above basal levels do have the potential to further shift channel activation gating. Thus, we find that HCN2 rundown upon patch excision is associated with a ~40-mV hyperpolarizing voltage shift in gating. Up to 20 mV of this shift can be attributed to the loss of the facilitatory action of basal levels of cAMP [11], suggesting that PI(4,5)P$_2$ hydrolysis upon patch excision can shift gating by ~20 mV. In contrast, we found that direct application of 1 μM of PI(4,5)P$_2$ to HCN channels in inside-out patches produced a ~32-mV depolarizing shift in gating [51]. Furthermore, one patch exposed to 10 μM PI(4,5)P$_2$ exhibited a >50-mV depolarizing shift in the HCN2 activation curve (Pian and Siegelbaum, unpublished results). If resting levels of PI(4,5)P$_2$ were saturating, then exogenous application of the phospholipid should produce at most a +20-mV voltage shift, precisely countering the effect of rundown.

The idea that bradykinin is capable of enhancing PI(4,5)P$_2$ synthesis is also consistent with previous studies. Thus, Gamper et al. [19] found that muscarinic M1 receptor activation exerted an inhibitory effect on N-type voltage-gated Ca^{2+} channels in sympathetic neurons because of a PLC-mediated decrease in PI(4,5)P$_2$ levels. In contrast, bradykinin produced little inhibitory effect through this mechanism, even though it stimulated PLC activity similar to M1 agonists. However, Gamper et al. reported that upon blockade of PI kinase activity with wortmannin, the ability of bradykinin to inhibit Ca^{2+} current through PI(4,5)P$_2$ hydrolysis was greatly enhanced. These findings led Gamper et al. to propose that bradykinin normally stimulates PI(4,5)P$_2$ synthesis in addition to activating PLC, thus causing little net change in PI(4,5)P$_2$ levels.

A study by Hughes et al. [29] in this issue of the European Journal of Physiology provides additional support for the view that bradykinin enhances PI(4,5)P$_2$ production. These authors used a fluorescently tagged PI(4,5)P$_2$-binding protein to monitor membrane levels of this phospholipid in sympathetic neurons after receptor stimulation. In agreement with the findings of Gamper et al., bradykinin produced significantly less translocation of the PI(4,5)P$_2$-reporter compared to that seen in response to an M1 agonist. Inhibition of PI(4,5)P$_2$ synthesis greatly increased the effect of bradykinin to translocate the reporter construct, again suggesting that BK$_2$ receptor activation leads to a stimulation of PI(4,5)P$_2$ synthesis that counteracts the normal decrease in PI(4,5)P$_2$ levels associated with PLC activation.

Given our experimental observations and these previous findings, we believe that the most parsimonious mechanism for the modulatory effects on HCN channel gating we observed in response to the receptor-dependent stimulation of PLC activity involves a net increase in local PI(4,5)P$_2$ levels near the HCN channels caused by an increase in PI(4,5)P$_2$ synthesis. Although we cannot rule out all alternative mechanisms, our experiments indicate that such mechanisms do not involve the canonical signaling pathways downstream of PLC.

How might activation of PLC stimulate PI(4,5)P$_2$ synthesis? In the heart, activation of PLC increases PI(4,5)P$_2$ synthesis as a result of the IP$_3$-dependent release of Ca^{2+} from intracellular stores [58]. More recently, neuronal calcium sensor-1 (NCS-1) was shown to stimulate PI 4-kinase in a Ca^{2+}-dependent manner [19, 24, 77, 89, 90]. An increase in cytoplasmic Ca^{2+}, however, is not likely to mediate the increase in PI(4,5)P$_2$ in our experiments as chelation of intracellular Ca^{2+} by BAPTA did not block channel modulation (although we cannot rule out the possibility that some residual Ca^{2+} increase was still present). Phosphatidic acid (PA), produced from DAG by DAG kinases, has been found to stimulate PI(4,5)P$_2$ synthesis by enhancing both PI 4-kinase and type I PI 5-kinase activity [28, 40]. However, activation of DAG kinases is blocked by calphostin C [60] and R59949, and neither inhibitor altered the modulation of HCN2. Thus, although an increase in PI(4,5)P$_2$ provides the simplest explanation of our results, it remains unclear how this increase might occur.

Potential physiological relevance of HCN channel modulation by PLC-linked receptors

The modulatory effects of PLC-linked receptor-stimulation on HCN channel function that we observe in *Xenopus* oocytes are comparable to or even greater than the magnitude of the classical effects of cAMP to shift HCN gating to more positive voltages. This novel PLC-dependent and cAMP-independent modulatory mechanism could therefore produce dramatic changes in cellular electrical activity that involve I$_h$, including an acceleration of heart rate, changes in neuronal spontaneous firing, and alterations in the dendritic integration of synaptic potentials.

Given the large number of receptors linked to phospholipase C and their universal expression, this form of modulation could potentially occur in a wide range of cells that express HCN channels. Indeed, depolarizing shifts in the gating of I$_h$ have been observed after the activation of several receptors coupled to PLC in various classes of neurons. For example, positive voltage shifts in activation gating of I$_h$ were observed after stimulation of the H$_2$ histamine receptor (+7.6 mV) and M3 muscarinic receptor

(+5 mV) in neurons of the thalamic lateral geniculate nucleus [43, 91]. Positive shifts were also reported upon activation of the AT_1 angiotensin receptor (+8.1 mV) and NMU-2 neuromedin receptor (+10.8 mV) in parvocellular neurons of the hypothalamic paraventricular nucleus [16, 53, 54]. In other neurons, activation of receptors coupled to PLC reduced HCN current amplitude, similar to that seen in our experiments in response to bradykinin or NGF. For example, TrkB receptor activation in neurons of the pre-Botzinger complex [69] and $5-HT_2$ receptor activation in dopaminergic neurons of the ventral tegmental area reduced I_h by 45–50% [38]. However, none of the above modulatory actions involved both a depolarizing shift in the $V_{1/2}$ of voltage gating and a reduction in I_h amplitude, the hallmark of the effects we observed upon PLC stimulation with BK_2 or TrkA receptor activation.

In addition to producing positive shifts in HCN channel gating, activation of receptors coupled to PLC can elicit hyperpolarizing shifts in I_h activation in other neurons, suggesting that receptor-mediated decreases in $PI(4,5)P_2$ levels may be able to produce the expected action to inhibit HCN channel gating under some circumstances. For example, stimulation of NK1 receptors by substance P in vagal sensory neurons produced a 20-mV hyperpolarizing shift in the activation of native I_h [30]. In cerebellar Purkinje neurons, activation of $5-HT_{2A}$ and $5-HT_{2C}$ receptors, which are both coupled to $G_{q/11}$ [33], also led to a hyperpolarizing shift in HCN current activation [37]. Finally, in neurons of the pre-Botzinger complex, TrkB receptor stimulation by brain-derived neurotrophic factor (BDNF) also caused a large hyperpolarizing shift in I_h gating [69].

The variability in the modulatory effects on HCN channel function in different cells upon activation of receptors coupled to PLC could reflect the differential ability of these receptors to couple to distinct lipid metabolic pathways in different cells. Even using heterologous expression of recombinant receptors and channels in oocytes, we found a heterogeneity in PLC-dependent receptor actions, with BK_2, TrkA, and M1 ACh receptors all leading to a positive shift in HCN channel voltage gating through a PI kinase-dependent mechanism, but only BK_2 and TrkA receptors capable of producing a PI kinase-independent decrease in maximal current amplitude. This heterogeneity raises the interesting possibility that the stimulation of a given PLC-coupled receptor could either decrease or increase cellular excitability depending on the metabolic state of the cell through the differential regulation of HCN channel function. It will thus be important in the future to reinvestigate previously reported modulatory actions on HCN channel function to determine whether receptor-mediated changes in $PI(4,5)P_2$ levels provide a general, but previously unrecognized, mechanism for flexibly altering HCN channel activity in a wide range of cells.

References

1. Arcaro A, Wymann MP (1993) Wortmannin is a potent phosphatidylinositol 3-kinase inhibitor: the role of phosphatidylinositol 3,4,5-trisphosphate in neutrophil responses. Biochem J 296(Pt 2):297–301

2. Arinsburg SS, Cohen IS, Yu HG (2006) Constitutively active Src tyrosine kinase changes gating of HCN4 channels through direct binding to the channel proteins. J Cardiovasc Pharmacol 47:578–586

3. Balla A, Balla T (2006) Phosphatidylinositol 4-kinases: old enzymes with emerging functions. Trends Cell Biol 16:351–361

4. Barbuti A, Gravante B, Riolfo M, Milanesi R, Terragni B, DiFrancesco D (2004) Localization of pacemaker channels in lipid rafts regulates channel kinetics. Circ Res 94:1325–1331

5. Barbuti A, Terragni B, Brioschi C, Difrancesco D (2007) Localization of f-channels to caveolae mediates specific beta(2)-adrenergic receptor modulation of rate in sinoatrial myocytes. J Mol Cell Cardiol 42:71–78

6. Baron CB, Pompeo J, Blackman D, Coburn RF (1993) Common phosphatidylinositol 4,5-bisphosphate pools are involved in carbachol and serotonin activation of tracheal smooth muscle. J Pharmacol Exp Ther 266:8–15

7. Berridge MJ (1984) Inositol trisphosphate and diacylglycerol as second messengers. Biochem J 220:345–360

8. Brose N, Betz A, Wegmeyer H (2004) Divergent and convergent signaling by the diacylglycerol second messenger pathway in mammals. Curr Opin Neurobiol 14:328–340

9. Cathala L, Paupardin-Tritsch D (1997) Neurotensin inhibition of the hyperpolarization-activated cation current (Ih) in the rat substantia nigra pars compacta implicates the protein kinase C pathway. J Physiol 503(Pt 1):87–97

10. Chang F, Cohen IS, DiFrancesco D, Rosen MR, Tromba C (1991) Effects of protein kinase inhibitors on canine Purkinje fibre pacemaker depolarization and the pacemaker current if. J Physiol 440:367–384

11. Chen S, Wang J, Siegelbaum SA (2001) Properties of hyperpolarization-activated pacemaker current defined by coassembly of HCN1 and HCN2 subunits and basal modulation by cyclic nucleotide. J Gen Physiol 117:491–504

12. Chen TY, Yau KW (1994) Direct modulation by Ca(2+)-calmodulin of cyclic nucleotide-activated channel of rat olfactory receptor neurons. Nature 368:545–548

13. Chuang HH, Prescott ED, Kong H, Shields S, Jordt SE, Basbaum AI, Chao MV, Julius D (2001) Bradykinin and nerve growth factor release the capsaicin receptor from PtdIns(4,5)P2-mediated inhibition. Nature 411:957–962

14. Craven KB, Zagotta WN (2006) CNG and HCN channels: two peas, one pod. Annu Rev Physiol 68:375–401

15. DiFrancesco D, Ferroni A, Mazzanti M, Tromba C (1986) Properties of the hyperpolarizing-activated current (if) in cells isolated from the rabbit sino-atrial node. J Physiol 377:61–88

16. Egli M, Berger T, Imboden H (2002) Angiotensin II influences the hyperpolarization-activated current Ih in neurones of the rat paraventricular nucleus. Neurosci Lett 330:53–56

17. Fogle KJ, Lyashchenko AK, Turbendian HK, Tibbs GR (2007) HCN pacemaker channel activation is controlled by acidic lipids downstream of diacylglycerol kinase and phospholipase A2. J Neurosci 27:2802–2814

18. Furuichi T, Yoshikawa S, Miyawaki A, Wada K, Maeda N, Mikoshiba K (1989) Primary structure and functional expression of the inositol 1,4,5-trisphosphate-binding protein P400. Nature 342:32–38

19. Gamper N, Reznikov V, Yamada Y, Yang J, Shapiro MS (2004) Phosphatidylinositol [correction] 4,5-bisphosphate signals underlie receptor-specific Gq/11-mediated modulation of N-type Ca2+ channels. J Neurosci 24:10980–10992

20. Gerber U, Gee CE, Benquet P (2007) Metabotropic glutamate receptors: intracellular signaling pathways. Curr Opin Pharmacol 7:56–61

21. Gomez-Hernandez JM, Stuhmer W, Parekh AB (1997) Calcium dependence and distribution of calcium-activated chloride channels in Xenopus oocytes. J Physiol 502(Pt 3):569–574

22. Goulding EH, Ngai J, Kramer RH, Colicos S, Axel R, Siegelbaum SA, Chess A (1992) Molecular cloning and single-channel properties of the cyclic nucleotide-gated channel from catfish olfactory neurons. Neuron 8:45–58

23. Hagiwara N, Irisawa H (1989) Modulation by intracellular Ca2+ of the hyperpolarization-activated inward current in rabbit single sino-atrial node cells. J Physiol 409:121–141

24. Hendricks KB, Wang BQ, Schnieders EA, Thorner J (1999) Yeast homologue of neuronal frequenin is a regulator of phosphatidylinositol-4-OH kinase. Nat Cell Biol 1:234–241

25. Hilgemann DW, Ball R (1996) Regulation of cardiac Na+,Ca2+ exchange and KATP potassium channels by PIP2. Science 273:956–959

26. Hilgemann DW, Feng S, Nasuhoglu C (2001) The complex and intriguing lives of PIP2 with ion channels and transporters. Sci Signal Transduct Knowl Environ 2001:RE19

27. Hofmann T, Obukhov AG, Schaefer M, Harteneck C, Gudermann T, Schultz G (1999) Direct activation of human TRPC6 and TRPC3 channels by diacylglycerol. Nature 397:259–263

28. Honda A, Nogami M, Yokozeki T, Yamazaki M, Nakamura H, Watanabe H, Kawamoto K, Nakayama K, Morris AJ, Frohman MA, Kanaho Y (1999) Phosphatidylinositol 4-phosphate 5-kinase alpha is a downstream effector of the small G protein ARF6 in membrane ruffle formation. Cell 99:521–532

29. Hughes S, Marsh SJ, Tinker A, Brown DA (2007) PIP2-dependent inhibition of M-type (Kv7.2/7.3) potassium channels: direct on-line assessment of PIP2 depletion by Gq-coupled receptors in single living neurons. Pflugers Arch (in press)

30. Jafri MS, Weinreich D (1998) Substance P regulates Ih via a NK-1 receptor in vagal sensory neurons of the ferret. J Neurophysiol 79:769–777

31. Kiss Z, Farkas T (1975) The effect of isoproterenol on the metabolism of phosphatidylinositol by rat heart in vitro. Biochem Pharmacol 24:999–1002

32. Kobrinsky E, Mirshahi T, Zhang H, Jin T, Logothetis DE (2000) Receptor-mediated hydrolysis of plasma membrane messenger PIP2 leads to K+-current desensitization. Nat Cell Biol 2:507–514

33. Kroeze WK, Kristiansen K, Roth BL (2002) Molecular biology of serotonin receptors structure and function at the molecular level. Curr Top Med Chem 2:507–528

34. Lambert S, Vind-Kezunovic D, Karvinen S, Gniadecki R (2006) Ligand-independent activation of the EGFR by lipid raft disruption. J Invest Dermatol 126:954–962

35. Lassing I, Lindberg U (1990) Polyphosphoinositide synthesis in platelets stimulated with low concentrations of thrombin is enhanced before the activation of phospholipase C. FEBS Lett 262:231–233

36. Lei Q, Jones MB, Talley EM, Garrison JC, Bayliss DA (2003) Molecular mechanisms mediating inhibition of G protein-coupled inwardly rectifying K+ channels. Mol Cells 15:1–9

37. Li SJ, Wang Y, Strahlendorf HK, Strahlendorf JC (1993) Serotonin alters an inwardly rectifying current (Ih) in rat

38. Liu Z, Bunney EB, Appel SB, Brodie MS (2003) Serotonin reduces the hyperpolarization-activated current (Ih) in ventral tegmental area dopamine neurons: involvement of 5-HT2 receptors and protein kinase C. J Neurophysiol 90:3201–3212

39. Loeb DM, Stephens RM, Copeland T, Kaplan DR, Greene LA (1994) A Trk nerve growth factor (NGF) receptor point mutation affecting interaction with phospholipase C-gamma 1 abolishes NGF-promoted peripherin induction but not neurite outgrowth. J Biol Chem 269:8901–8910

40. Luo B, Prescott SM, Topham MK (2004) Diacylglycerol kinase zeta regulates phosphatidylinositol 4-phosphate 5-kinase Ialpha by a novel mechanism. Cell Signal 16:891–897

41. Luthi A, McCormick DA (1999) Modulation of a pacemaker current through Ca(2+)-induced stimulation of cAMP production. Nat Neurosci 2:634–641

42. Maeno-Hikichi Y, Chang S, Matsumura K, Lai M, Lin H, Nakagawa N, Kuroda S, Zhang JF (2003) A PKC epsilon-ENH-channel complex specifically modulates N-type Ca2+ channels. Nat Neurosci 6:468–475

43. McCormick DA, Williamson A (1991) Modulation of neuronal firing mode in cat and guinea pig LGNd by histamine: possible cellular mechanisms of histaminergic control of arousal. J Neurosci 11:3188–3199

44. Meakin SO, MacDonald JI, Gryz EA, Kubu CJ, Verdi JM (1999) The signaling adapter FRS-2 competes with Shc for binding to the nerve growth factor receptor TrkA. A model for discriminating proliferation and differentiation. J Biol Chem 274:9861–9870

45. Meyers R, Cantley LC (1997) Cloning and characterization of a wortmannin-sensitive human phosphatidylinositol 4-kinase. J Biol Chem 272:4384–4390

46. Mignery GA, Newton CL, Archer BT 3rd, Sudhof TC (1990) Structure and expression of the rat inositol 1,4,5-trisphosphate receptor. J Biol Chem 265:12679–12685

47. Mikoshiba K, Hattori M (2000) IP3 receptor-operated calcium entry. Sci Signal Transduct Knowl Environ 2000:PE1

48. Nakanishi S, Catt KJ, Balla T (1995) A wortmannin-sensitive phosphatidylinositol 4-kinase that regulates hormone-sensitive pools of inositolphospholipids. Proc Natl Acad Sci USA 92:5317–5321

49. Nasuhoglu C, Feng S, Mao Y, Shammat I, Yamamato M, Earnest S, Lemmon M, Hilgemann DW (2002) Modulation of cardiac PIP2 by cardioactive hormones and other physiologically relevant interventions. Am J Physiol Cell Physiol 283:C223–C234

50. Patel S, Joseph SK, Thomas AP (1999) Molecular properties of inositol 1,4,5-trisphosphate receptors. Cell Calcium 25:247–264

51. Pian P, Bucchi A, Robinson RB, Siegelbaum SA (2006) Regulation of gating and rundown of HCN hyperpolarization-activated channels by exogenous and endogenous PIP2. J Gen Physiol 128:593–604

52. Poolos NP, Bullis JB, Roth MK (2006) Modulation of h-channels in hippocampal pyramidal neurons by p38 mitogen-activated protein kinase. J Neurosci 26:7995–8003

53. Qiu DL, Chu CP, Shirasaka T, Nabekura T, Kunitake T, Kato K, Nakazato M, Katoh T, Kannan H (2003) Neuromedin U depolarizes rat hypothalamic paraventricular nucleus neurons in vitro by enhancing IH channel activity. J Neurophysiol 90:843–850

54. Qiu DL, Chu CP, Tsukino H, Shirasaka T, Nakao H, Kato K, Kunitake T, Katoh T, Kannan H (2005) Neuromedin U receptor-2 mRNA and HCN channels mRNA expression in NMU-sensitive neurons in rat hypothalamic paraventricular nucleus. Neurosci Lett 374:69–72

cerebellar Purkinje cells under voltage clamp. Brain Res 617:87–95

55. Quist E, Sanchez M (1983) Alpha adrenergic drugs induce a phospholipid effect in canine heart. Proc West Pharmacol Soc 26:333–335

56. Quist E, Satumtira N, Powell P (1989) Regulation of polyphosphoinositide synthesis in cardiac membranes. Arch Biochem Biophys 271:21–32

57. Quist EE (1982) Evidence for a carbachol stimulated phosphatidylinositol effect in heart. Biochem Pharmacol 31:3130–3133

58. Quist EE, Satumtira N (1987) Muscarinic receptor stimulated phosphoinositide turnover in cardiac atrial tissue. Biochem Pharmacol 36:499–505

59. Ranganathan R, Malicki DM, Zuker CS (1995) Signal transduction in Drosophila photoreceptors. Annu Rev Neurosci 18:283–317

60. Redman R, Lefevre J, MacDonald ML (1995) Inhibition of diacylglycerol kinase by the antitumor agent calphostin C. Evidence for similarity between the active site of diacylglycerol kinase and the regulatory site of protein kinase C. Biochem Pharmacol 50:235–241

61. Robinson RB, Siegelbaum SA (2003) Hyperpolarization-activated cation currents: from molecules to physiological function. Annu Rev Physiol 65:453–480

62. Sekar MC, Roufogalis BD (1984) Comparison of muscarinic and alpha-adrenergic receptors in rat atria based on phosphoinositide turnover. Life Sci 35:1527–1533

63. Snow P, Yim DL, Leibow JD, Saini S, Nuccitelli R (1996) Fertilization stimulates an increase in inositol trisphosphate and inositol lipid levels in Xenopus eggs. Dev Biol 180:108–118

64. Song DK, Ashcroft FM (2001) ATP modulation of ATP-sensitive potassium channel ATP sensitivity varies with the type of SUR subunit. J Biol Chem 276:7143–7149

65. Suh BC, Hille B (2002) Recovery from muscarinic modulation of M current channels requires phosphatidylinositol 4,5-bisphosphate synthesis. Neuron 35:507–520

66. Suh BC, Hille B (2005) Regulation of ion channels by phosphatidylinositol 4,5-bisphosphate. Curr Opin Neurobiol 15:370–378

67. Suh BC, Inoue T, Meyer T, Hille B (2006) Rapid chemically induced changes of PtdIns(4,5)P2 gate KCNQ ion channels. Science 314(5804):1454–1457

68. Sul D, Baron CB, Broome R, Coburn RF (2001) Smooth muscle length-dependent PI(4,5)P2 synthesis and paxillin tyrosine phosphorylation. Am J Physiol Cell Physiol 281:C300–C310

69. Thoby-Brisson M, Cauli B, Champagnat J, Fortin G, Katz DM (2003) Expression of functional tyrosine kinase B receptors by rhythmically active respiratory neurons in the pre-Botzinger complex of neonatal mice. J Neurosci 23:7685–7689

70. Thompson AK, Mostafapour SP, Denlinger LC, Bleasdale JE, Fisher SK (1991) The aminosteroid U-73122 inhibits muscarinic receptor sequestration and phosphoinositide hydrolysis in SK-N-SH neuroblastoma cells. A role for Gp in receptor compartmentation. J Biol Chem 266:23856–23862

71. Topham MK (2006) Signaling roles of diacylglycerol kinases. J Cell Biochem 97:474–484

72. Trudeau MC, Zagotta WN (2002) Mechanism of calcium/calmodulin inhibition of rod cyclic nucleotide-gated channels. Proc Natl Acad Sci USA 99:8424–8429

73. Vargas G, Lucero MT (2002) Modulation by PKA of the hyperpolarization-activated current (Ih) in cultured rat olfactory receptor neurons. J Membr Biol 188:115–125

74. Vazquez G, Wedel BJ, Aziz O, Trebak M, Putney JW Jr (2004) The mammalian TRPC cation channels. Biochim Biophys Acta 1742:21–36

75. Violin JD, Newton AC (2003) Pathway illuminated: visualizing protein kinase C signaling. IUBMB Life 55:653–660

76. Vlahos CJ, Matter WF, Hui KY, Brown RF (1994) A specific inhibitor of phosphatidylinositol 3-kinase, 2-(4-morpholinyl)-8-phenyl-4H-1-benzopyran-4-one (LY294002). J Biol Chem 269:5241–5248

77. Weisz OA, Gibson GA, Leung SM, Roder J, Jeromin A (2000) Overexpression of frequenin, a modulator of phosphatidylinositol 4-kinase, inhibits biosynthetic delivery of an apical protein in polarized madin-darby canine kidney cells. J Biol Chem 275:24341–24347

78. Wiesmann C, de Vos AM (2001) Nerve growth factor: structure and function. Cell Mol Life Sci 58:748–759

79. Winks JS, Hughes S, Filippov AK, Tatulian L, Abogadie FC, Brown DA, Marsh SJ (2005) Relationship between membrane phosphatidylinositol-4,5-bisphosphate and receptor-mediated inhibition of native neuronal M channels. J Neurosci 25:3400–3413

80. Womack KB, Gordon SE, He F, Wensel TG, Lu CC, Hilgemann DW (2000) Do phosphatidylinositides modulate vertebrate phototransduction? J Neurosci 20:2792–2799

81. Wu JY, Cohen IS (1997) Tyrosine kinase inhibition reduces i(f) in rabbit sinoatrial node myocytes. Pflugers Arch 434:509–514

82. Wu L, Bauer CS, Zhen XG, Xie C, Yang J (2002) Dual regulation of voltage-gated calcium channels by PtdIns(4,5)P2. Nature 419:947–952

83. Xu C, Watras J, Loew LM (2003) Kinetic analysis of receptor-activated phosphoinositide turnover. J Cell Biol 161:779–791

84. Yu H, Chang F, Cohen IS (1995) Pacemaker current i(f) in adult canine cardiac ventricular myocytes. J Physiol 485(Pt 2):469–483

85. Yu HG, Lu Z, Pan Z, Cohen IS (2004) Tyrosine kinase inhibition differentially regulates heterologously expressed HCN channels. Pflugers Arch 447:392–400

86. Zhainazarov AB, Spehr M, Wetzel CH, Hatt H, Ache BW (2004) Modulation of the olfactory CNG channel by Ptdlns(3,4,5)P3. J Membr Biol 201:51–57

87. Zhang H, Craciun LC, Mirshahi T, Rohacs T, Lopes CM, Jin T, Logothetis DE (2003) PIP(2) activates KCNQ channels, and its hydrolysis underlies receptor-mediated inhibition of M currents. Neuron 37:963–975

88. Zhang H, He C, Yan X, Mirshahi T, Logothetis DE (1999) Activation of inwardly rectifying K+ channels by distinct PtdIns (4,5)P2 interactions. Nat Cell Biol 1:183–188

89. Zhao X, Varnai P, Tuymetova G, Balla A, Toth ZE, Oker-Blom C, Roder J, Jeromin A, Balla T (2001) Interaction of neuronal calcium sensor-1 (NCS-1) with phosphatidylinositol 4-kinase beta stimulates lipid kinase activity and affects membrane trafficking in COS-7 cells. J Biol Chem 276:40183–40189

90. Zheng Q, Bobich JA, Vidugiriene J, McFadden SC, Thomas F, Roder J, Jeromin A (2005) Neuronal calcium sensor-1 facilitates neuronal exocytosis through phosphatidylinositol 4-kinase. J Neurochem 92:442–451

91. Zhu JJ, Uhlrich DJ (1998) Cellular mechanisms underlying two muscarinic receptor-mediated depolarizing responses in relay cells of the rat lateral geniculate nucleus. Neuroscience 87:767–781

92. Zolles G, Klocker N, Wenzel D, Weisser-Thomas J, Fleischmann BK, Roeper J, Fakler B (2006) Pacemaking by HCN channels requires interaction with phosphoinositides. Neuron 52:1027–1036

93. Zong X, Eckert C, Yuan H, Wahl-Schott C, Abicht H, Fang L, Li R, Mistrik P, Gerstner A, Much B, Baumann L, Michalakis S, Zeng R, Chen Z, Biel M (2005) A novel mechanism of modulation of hyperpolarization-activated cyclic nucleotide-gated channels by Src kinase. J Biol Chem 280:34224–34232